

GASIFICATION OF CAKING COAL IN A FREE-FALL, FLUID-BED REACTOR

A. J. Forney, R. F. Kenny, and J. H. Field

Pittsburgh Coal Research Center, U. S. Bureau of Mines,
4800 Forbes Avenue, Pittsburgh, Pennsylvania 15213

INTRODUCTION

The Bureau of Mines is investigating the gasification of caking coals in a fluid-bed reactor as part of the Bureau's overall program of converting coal to liquid or gaseous fuels. The caking coals, common to the East and Midwest, cannot be gasified without being pretreated, usually with steam and oxygen. The method of gasification discussed in this report is free-fall pretreatment combined with fluid-bed gasification.

The primary objectives of the project are: 1) To check our earlier method of pretreating caking coals before gasification;^{2, 3/} 2) to determine the minimum amount of oxygen needed for pretreatment; 3) to maximize the methane content in the product gas. A secondary aim, which developed from the above tests, is to study a method of substituting air for oxygen.

EXPERIMENTAL PROCEDURE

The pretreatment is achieved by dropping Pittsburgh-seam coal (70 percent through 200 mesh) through a free-fall reactor 6 inches in diameter and 10 feet high (later reduced to 7 feet). This pretreater is located above a fluid-bed reactor 3 inches in diameter and 3 feet high (later increased to 6 feet). The oxygen and steam for the gasification enter the bottom of the reactor, figures 1 and 2. The gases from the gasifier flow up through the free-fall section to pretreat and carbonize the coal as it falls. They are enriched with an oxygen-steam feed entering the side of the free-fall section to further pretreat the coal because the gases rising from the gasifier did not pretreat sufficiently to prevent agglomeration.

Pressures from 2.5 to 20 atmospheres, temperatures of 835° to 955° C, and oxygen-coal ratios from 0 to 5.9 were used.

RESULTS AND DISCUSSION

Pressure Effects

The pressure was gradually increased from 2-1/2 to 20 atmospheres as shown in table 1 and figure 3. The methane content gradually increased to 14 volume percent of the product gas. This means that more methane can be produced in this gasification than would be produced in subsequent methanation to produce high-Btu gas. For example, in experiment N-12 the 50 percent H₂+CO would yield less methane during methanation than the 14 percent methane already produced in gasification. As the pressure was increased from 2-1/2 to 20 atmospheres,

figure 3, the percentage of methane in the product gas increased from 8 to 12, while the hydrogen and carbon monoxide percentages decreased. Also the carbon dioxide increased while the hydrogen and carbon monoxide decreased at the same rate, verifying Schuster's^{8/} claim that the methane-making reaction in gasification is $2\text{H}_2 + 2\text{CO} = \text{CH}_4 + \text{CO}_2$. These curves, figure 3, based on average values from several experiments are similar to those of O'Dell.^{4/}

Table 1.- Effect of Pressure on Methane Yield

Test No. ^{1/}	F-19	F-33	F-46	N-10	N-12	N-13	N-17
Pressure, atm	2.5	5	10	15	20	20	20
Coal ^{2/}	D-2	D-4	D-4	D-4	D-4	D-4	D-4
Coal feed, lb/hr	0.43	0.70	1.53	1.60	1.60	1.63	3.40
Input, SCFH:							
Gasifier, steam	18	25	50	60	60	60	100
Gasifier, oxygen	1	1.5	4	4	4	4	16
Pretreater, steam	10	10	20	30	30	20	20
Pretreater, oxygen	1	1.5	3	4	4	4	4
Nitrogen	4	4	8	6	6	5	5
Temperature, °C:							
Pretreater	375	409	390	375	400	400	400
Gasifier, avg	893	891	893	880	882	876	883
Gasifier, max	900	900	900	900	900	900	900
O ₂ /coal, SCF/lb	4.6	4.3	4.6	5.0	5.0	4.9	5.9
Steam/coal, SCF/lb	42	36	33	37	37	37	29
Carbon conversion, pct	67	68	60	66	65	73	68
Steam conversion, pct	12	10	15	17	14	23	--
Product gas, ^{3/} SCF/lb	19	19	16	17	15	18	16
Methane, SCF/lb	2.1	1.8	2.5	2.7	3.3	3.7	3.4
Product gas, pct:							
H ₂	44	41	39	39	34	36	35
CH ₄	8	7	11	11	14	14	14
CO	21	25	22	20	16	18	18
CO ₂	27	27	28	30	36	32	33
Tar, pct of coal feed	10	6	3	3	4	3	5

^{1/} F series with 3-foot reactor; N series with 6-foot reactor.

^{2/} D-2: H 5.1, C 72.9, N 1.4, O 8.2, S 1.3, Ash 11.1 percent.

D-4: H 5.1, C 76.5, N 1.5, O 8.1, S 1.0, Ash 8.0, VM 34.8 percent;
FSI = 7-1/2.

^{3/} H₂+CO+CH₄.

Tar Plus Oil

As the pressure increased the tar yield decreased from 10 to about 5 percent. The tars were analyzed by chromatography to find the effect of pressure on the composition of the tar. Results were inconclusive; no correlation could be made.

The coal feed rate was increased from 1.54 pounds per hour (33 lb/hr ft²) to 6.1 pounds per hour (133 lb/hr ft²) at 20 atmospheres pressure (table 2). The carbon conversion was lower at the higher coal rate. The methane yield was almost steady at 3 SCF/lb, although its percentage in the product gas increased from 12 to 15 percent.

Table 2.- Effect of Increased Coal Feed on Product Distribution
at 20 Atmospheres Pressure

Test No.	N-11	N-15	N-17	N-19	N-21	N-24	N-22	Lurgi ^{1/}
Coal ^{2/}	D-4	D-4	D-4	D-5	D-5	D-5	D-5	D-5
Feed, lb/hr	1.54	2.25	3.40	5.40	5.82	6.1	5.2	
Coal feed, lb/hr ft ²	33	49	74	120	127	133	113	
Coal feed, lb/hr ft ³	6	8	12	20	21	22	18	
Input, SCFH:								
Gasifier, steam	60	65	100	150	180	180	198	
Gasifier, oxygen	4	6	16	24	22	18	6	
Pretreater, steam ...	30	15	20	24	36	36	36	
Pretreater, oxygen ..	4	3	4	6	6	6	6	
Nitrogen	6	6	5	5	5	5	5	
Temperature, °C:								
Pretreater	375	400	400	400	400	400	400	
Gasifier, avg	889	885	883	907	864	890	889	
Gasifier, max	900	898	900	959	890	910	900	
O ₂ /coal, SCF/lb	5.2	4.0	5.9	5.6	4.8	4.0	2.3	4
Steam/coal, SCF/lb	39	29	29	28	31	30	38	19
Carbon conversion, pct ..	73	68	68	75	59	55	52	90 ^{3/}
Steam conversion, pct ...	14	28	21	29	12	12	15	
Product gas, ^{4/} SCF/lb	19	19	16	16	13	12	15	19
Methane, SCF/lb	3.2	3.3	3.4	3.2	3.0	2.7	3.2	2.6
Product gas, pct:								
H ₂	38	39	35	33	33	34	40	40
CH ₄	12	13	14	13	15	15	17	10
CO	21	23	18	19	16	18	18	25
CO ₂	29	25	33	35	36	33	25	25
Tar, pct of feed	4	4	5	9	4	3	3	

^{1/} Westfield plant coal: Moist. = 15.6, ash = 14.6, VM = 28.7, FC = 41.1 pct.

^{2/} D-4: H 5.1, C 76.5, N 1.4, O 8.1, S 1.0, Ash 8.0, VM 34.8 pct; FSI = 7-1/2.
D-5: H 5.0, C 74.9, N 1.5, O 7.6, S 1.1, Ash 9.9, VM 34.7 pct; FSI = 8-1/2.

^{3/} Estimated.

^{4/} H₂+CO+CH₄.

The results of N-23 (table 3) and N-19 (table 2) may be compared with those of the Westfield^{2/} Lurgi. Our methane percentage is higher, and our methane yield slightly higher. We used more oxygen and more steam and had a lower carbon conversion; however, the Lurgi could not be operated with the caking coal used in our tests.

Effect of Low Oxygen Feed

In test N-22 the oxygen feed to the gasifier was reduced from the 4 to 5 cubic feet per pound used in the other tests to 1 cubic foot per pound. Comparing test N-22 with N-19 shows that the carbon conversion decreased, the methane yield remained the same, but the percentage of methane in the product gas increased from 13 to 17 percent (table 2). This increase is desirable, but a commercial gasifier would have to be heated externally to operate with such a low oxygen feed.

Table 3.- Effect of Temperature on Product Distribution
at 20 Atmospheres Pressure

Test No.	N-26	N-25	N-24	N-27	N-23	N-28	N-30
Coal ^{1/}	D-6	D-6	D-5	D-6	D-6	D-6	D-6
Coal feed, lb/hr ft ²	123	136	133	140	133	140	136
Feed, lb/hr	5.65	6.25	6.1	6.5	6.0	6.4	6.3
Input, SCFH:							
Gasifier, steam	180	180	180	180	180	180	120
Gasifier, oxygen	18	18	18	18	24	18	18
Pretreater, steam	36	36	36	36	36	36	36
Pretreater, oxygen	6	6	6	6	6	6	6
Nitrogen	5	5	5	5	5	5	5
Temperature, °C:							
Pretreater	400	400	400	400	400	400	400
Gasifier, avg	835	860	890	880	900	901	912
Gasifier, max	857	880	910	910	955	934	963
Oxygen/coal, SCF/lb	4.3	3.8	4.0	3.7	5.0	3.8	3.8
Steam/coal, SCF/lb	32	29	30	28	30	28	19
Carbon conversion, pct	51	58	55	59	81	65	56
Steam conversion, pct	4	--	12	--	24	--	--
Product gas, ^{2/} SCF/lb	11	14	12	14	19	16	13
Methane, SCF/lb	2.5	2.9	2.7	3.5	3.6	3.2	2.9
Product gas, pct:							
H ₂	31	36	34	34	36	36	33
CH ₄	15	14	15	17	13	14	16
CO	20	17	18	17	20	20	18
CO ₂	34	33	33	32	31	30	33
Tar, pct of feed	7	8	3	4	3	5	4

^{1/} D-5: H 5.0, C 74.9, N 1.5, O 7.6, S 1.1, Ash 9.9, VM 34.7 pct; FSI = 8-1/2.

D-6: H 5.1, C 74.4, N 1.5, O 8.2, S 1.1, Ash 9.7, VM 36.1 pct; FSI = 8.

^{2/} H₂+CO+CH₄.

Effect of Temperature

For two reasons the temperature was not varied widely in these tests. The safe limit for the reactor at 20 atmospheres is 950° C and carbon conversion decreased markedly below 850° C. The yield of product gas increased from about 11 SCF of H₂+CO+CH₄ per pound of coal at 860° C to 19 at 950° C (table 3). The methane percentage decreased but not drastically. However, the yield of methane per pound coal feed did increase from 2.5 to 3.6 SCF per pound. In test N-30 the steam rate was reduced from 30 SCF per pound of coal to 19; the temperature increased in the gasifier but the carbon conversion dropped. Some sintering of the ash occurred at the base of the reactor, indicating that the flow of steam was too low. The optimum temperature seems to be about 900°-950° C. Further tests may be necessary to determine the maximum temperature because the methane yield may decrease so much at higher temperatures that the advantage of our method of operation may be lost.

Oxygen Needed for Pretreatment

Changing the port of entry for the pretreating steam and oxygen from the middle of the free-fall section, as shown in figure 1, to the top of the free-fall section reduced the amount of oxygen necessary for pretreatment. When the pretreating gases were fed at the top they entered through a tube surrounding the coal feed inlet port. Thus the coal was entrained by the treating gases for about 2 feet before it fell 5 feet into the fluid bed. In tables 1 and 2 the results of both systems represented by tests N-12 and N-24 are compared. The amount of oxygen needed for pretreatment was decreased from 2.5 SCF per pound (N-12) to less than 1 SCF per pound (N-24). When the pretreating steam and oxygen were fed at the middle of the free-fall section, some oxygen was used in gasification because of the high temperature in this zone. When they were fed at the top of the reactor, oxygen was used only for pretreatment.

Studies in Glass Equipment of a System Using Air Instead of Oxygen

Oxygen accounts for about 10 to 14 cents per MCF of the cost of making high-Btu gas. Many different systems have been tried both in England and America in the hope of substituting air for oxygen.^{1,5,6/} Our approach is to feed air and steam through separate entry ports to a single fluid bed so the products of combustion can be separated from the products of steam gasification. Two designs to achieve this are shown in figures 4 and 5, and glass models based on these designs have been made. The model similar to figure 4 is constructed with a straight baffle in a 6-inch-diameter glass tube; with an L/D ratio of 2 (12-inch height/6-inch diameter), the mixing of the air and inert gas streams is only 5 to 10 percent if the baffle extends 1 to 2 inches into the bed. When the baffle is raised above the bed, the mixing is 30 to 40 percent. When the ratio is 3, the mixing is about 25 percent. The second model similar to figure 5 was constructed with a 4-inch-diameter tube inserted into a 6-inch-diameter tube. The areas of the annulus and the inner tube are about the same. This model shows more mixing of the gases than the first--21 percent when the center tube is embedded 2 inches into a 6-inch layer of coal.

After a satisfactory model has been designed for gas flow, we will use a 6-inch-diameter steel reactor to study the mixing of the solids to determine if uniform temperatures in the bed can be obtained.

CONCLUSIONS

Caking coals can be gasified in a combined free-fall, fluid-bed gasifier. The methane in the product gas is about 14 to 15 percent, which means more methane is being produced in the gasification than would be produced in the subsequent methanation. The oxygen needed for pretreatment is about 1 cubic foot per pound coal feed.

A conceptual process being investigated substitutes air for oxygen during gasification.

BIBLIOGRAPHY

1. Curran, G. P., C. H. Rice, and E. Gorin. Carbon Dioxide Acceptor Gasification Process. Division of Fuel Chemistry, A.C.S., Philadelphia, Pa., April 5-10, 1964.
2. Forney, A. J., R. F. Kenny, S. J. Gasior, and J. H. Field. Fluid-Bed Gasification of Pretreated Pittsburgh-Seam Coal. Division of Fuel Chemistry, A.C.S., New York, N. Y., Sept. 1966.
3. Forney, A. J., R. F. Kenny, S. J. Gasior, and J. H. Field. Decaking of Coals in a Fluid Bed. BuMines Rept. of Inv. 6797, 1966, 22 pp.
4. O'Dell, W. W. Gasification of Solid Fuels in Germany by the Lurgi, Winkler and Leuna Slagging Type Gas Producer Processes. BuMines Inf. Circ. 7415, 1946, 46 pp.
5. Pieroni, L. J., G. T. Skaperdas, and W. H. Heffner. Development of the Kellogg Coal Gasification Process. A.I.Ch.E. Symposium on Processing of Coal and its Byproducts, Philadelphia, Pa., Dec. 5-9, 1965.
6. Raynor, J. W. R. Gasification by the Moving Burden Technique. Gasification and Liquefaction of Coal Symposium, A.I.M.E., New York, N. Y., Feb. 20-21, 1952.
7. Ricketts, T. S. The Operation of the Westfield Lurgi Plant and the High Pressure Grid System. The Institution of Gas Engineers 100th Annual General Meeting, May 1963, London, England.
8. Schuster, Fritz. The Chemical Reaction of Methane Formation in Oxygen-Pressure Gasification. Das Gas und Wasserfach 104 (49), 1963, pp. 1418-1419.

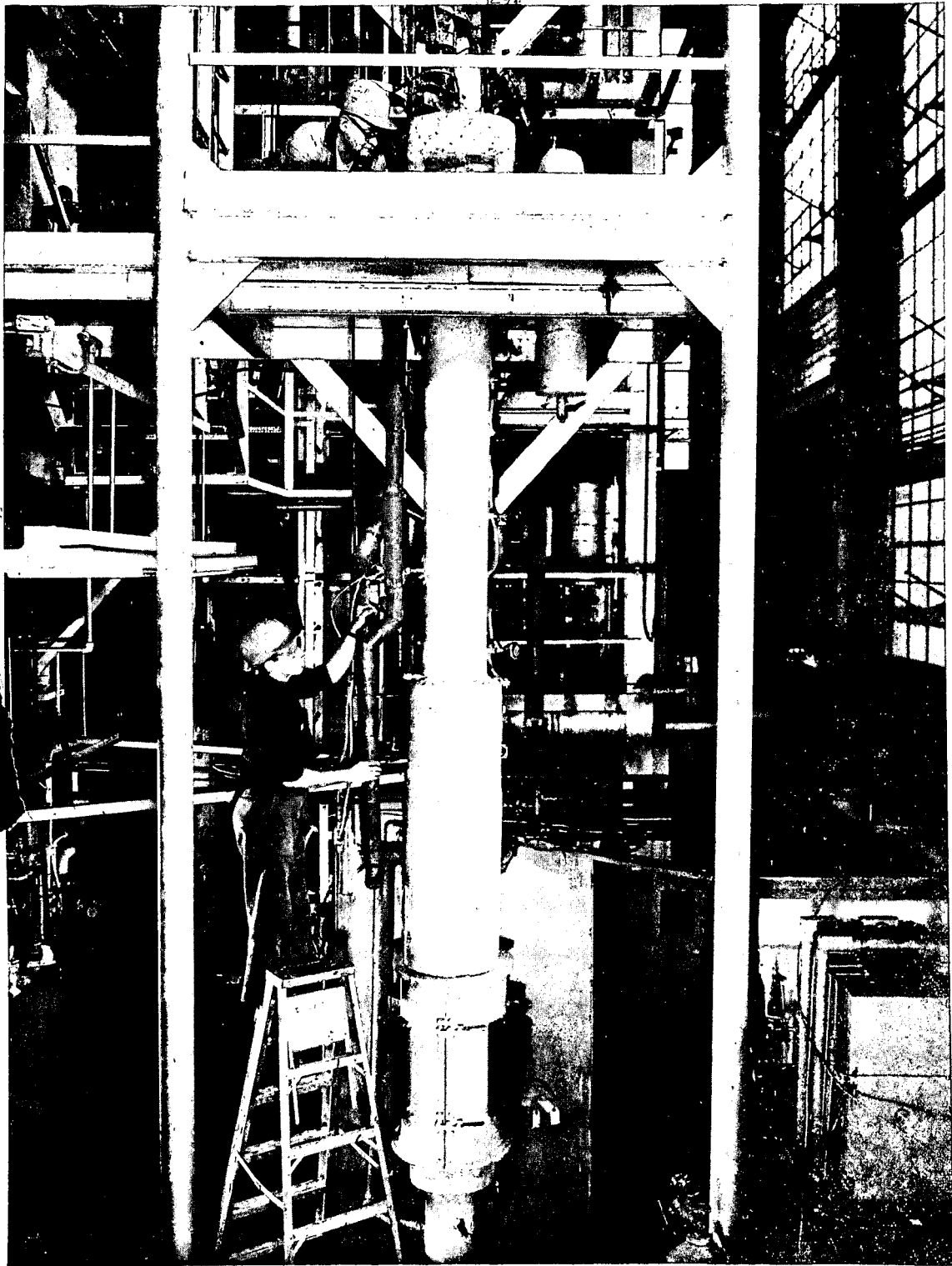


Figure 2. Gasification Equipment.

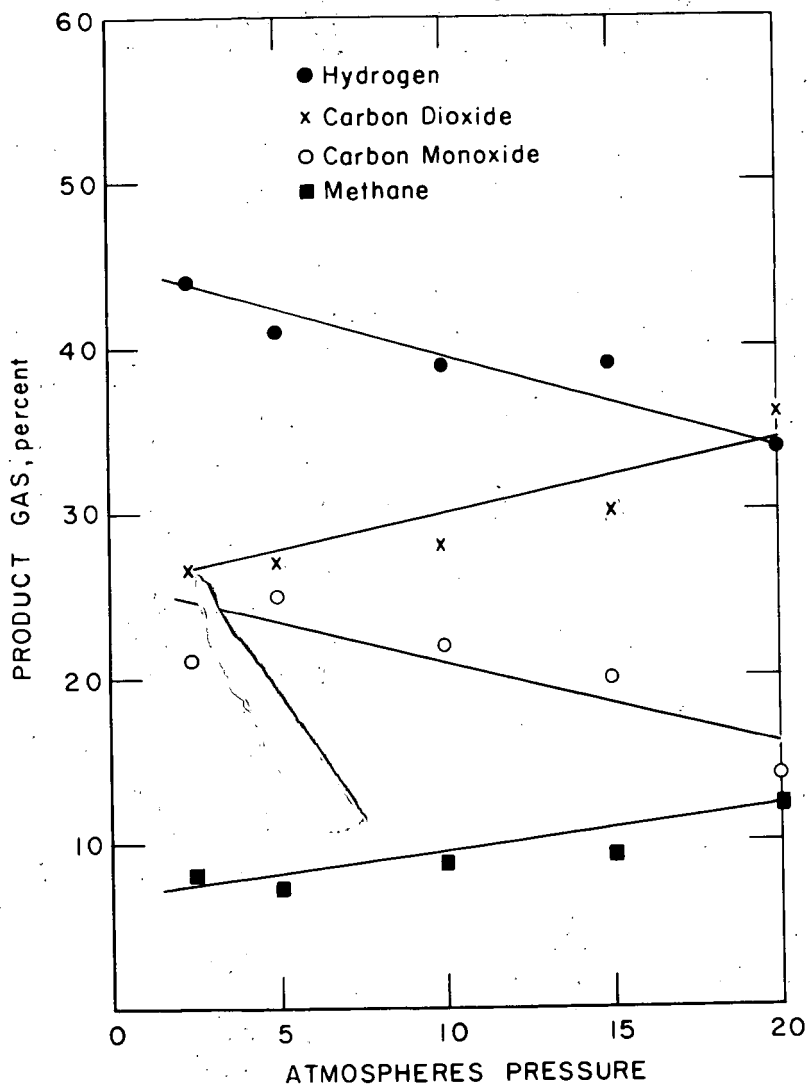


Figure 3.- Effect of pressure on the product gas.

4-13-67

L-9907

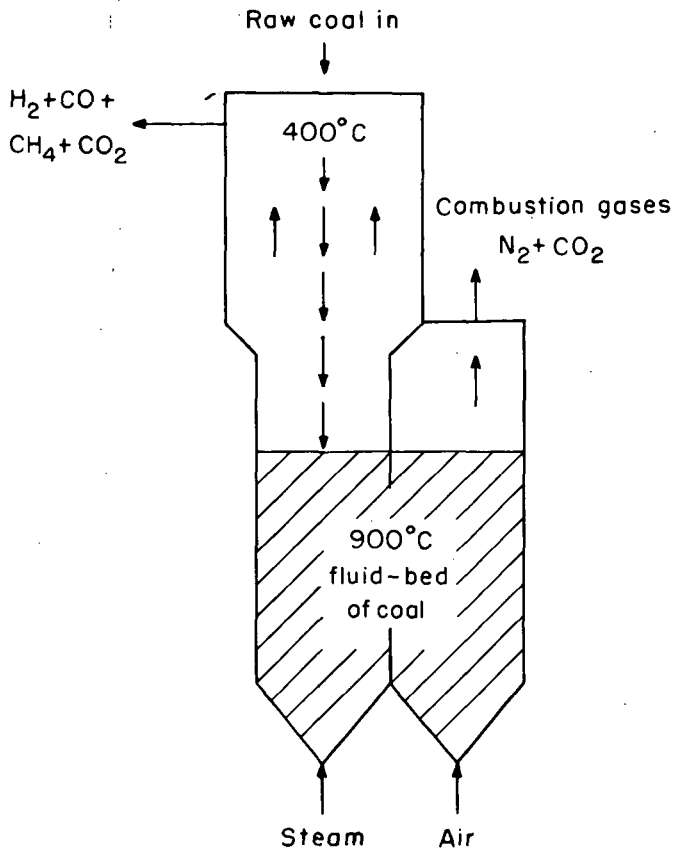


Figure 4 - Steam-coal, air-coal reaction in single fluid-bed gasifier

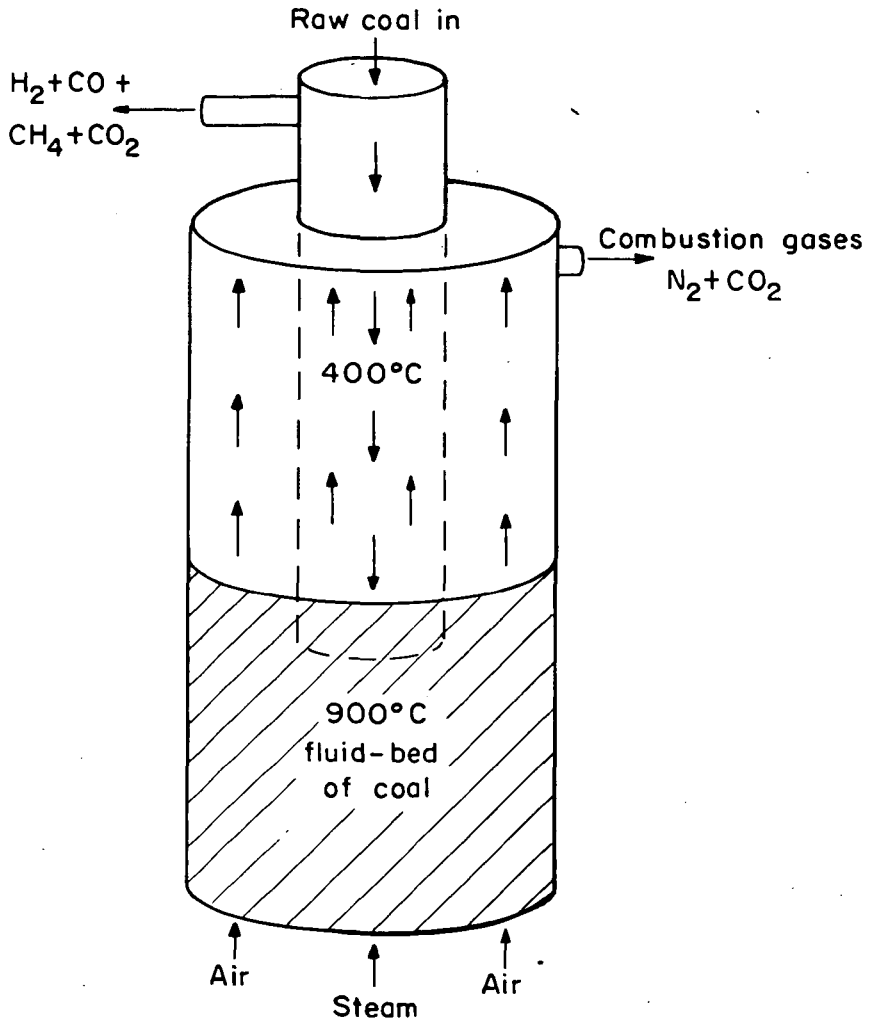


Figure 5.—Steam-coal, air-coal reaction in single fluid-bed gasifier.

4-5-67

L-9889

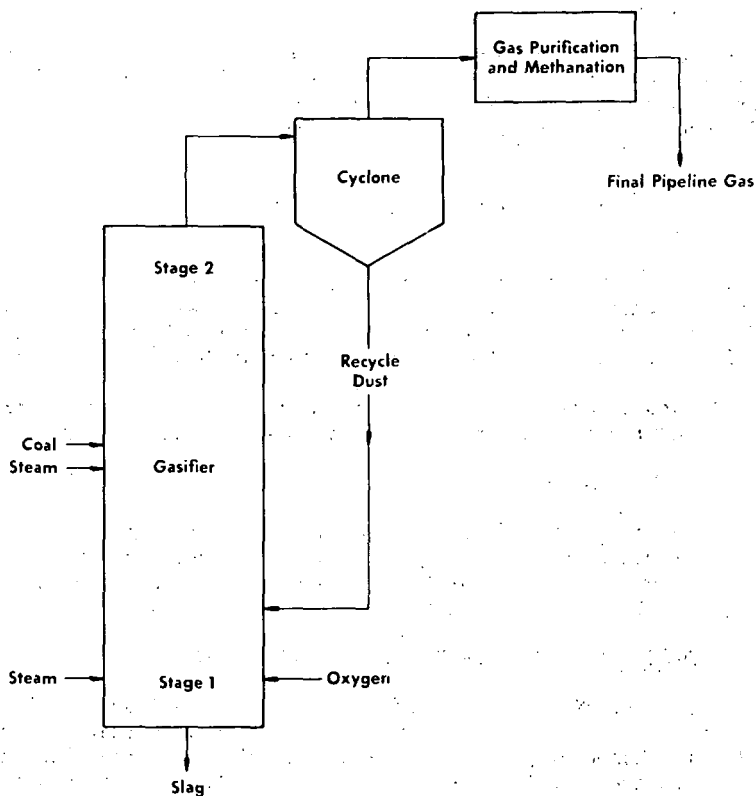
COMPUTER STUDY OF STAGE 2 REACTIONS IN THE BCR TWO-STAGE
SUPER-PRESSURE COAL GASIFICATION PROCESS

E. E. Donath and R. A. Glenn

Bituminous Coal Research, Inc., Monroeville, Pennsylvania

INTRODUCTION

In the BCR two-stage gasification process, recycle char is used in Stage 1 to produce hot synthesis gas by reaction with oxygen and steam. The hot products from Stage 1 heat the fresh coal and steam entering Stage 2 and react with them to produce methane and additional synthesis gas.(1,2)* A schematic flow diagram of the process is given as Figure 1.



8008G13

Figure 1. Simplified Flow Diagram for Two-stage
Super-pressure Gasifier

* Numbers in parenthesis refer to list of References at end of paper.

For the past two years, laboratory research has been under way to establish the optimum conditions for operation of Stage 2 of this conceptual process. Results of some of these experimental studies have already been reported.(3,4) This paper reports the results of a computer study of the thermochemistry of the two-stage process with emphasis on the effects of variations in the operating conditions. These data were needed: (a) to guide the experimental studies; and, (b) to indicate the corresponding effects of these variables on the final cost of pipeline gas as derived in the initial economic evaluation of the process.(1,2)

According to the initial economic evaluation of the overall process (1), the yield of methane produced directly from coal is of major importance for the economics of the process. In a study of the thermochemistry involved, consideration must be given to this reaction and means must be available for determining the extent it occurs.

At the time the study was begun, kinetic data for the rate of methane formation were not available; however, it was known that methane formation at the temperatures visualized for Stage 2 is a very rapid reaction (5), and that observed methane yields correspond to the thermodynamic equilibrium of the reaction



if an activity that varies from 1 to 3.4 is assumed for the carbon.(6)

Therefore, it was arbitrarily assumed for the present study that methane yields computed on this basis would be apt to respond to changes in Stage 2 temperature and pressure, and thus, they would be more realistic than selection of fixed methane yields. In addition, it was assumed that the rest of the carbon would be converted to CO + H₂ by reaction with steam and oxygen.

For the well known water-gas shift reaction, it was assumed that the reaction came to equilibrium at reaction temperature according to the equation:



For the evaluation of the effects of the various operating parameters, such as oxygen/coal ratio, steam/coal ratio, operating pressure, preheat temperatures, etc., one further assumption is necessary--namely, thermal equilibrium in each stage of the gasifier is achieved.

BASIS AND PROCEDURE FOR COMPUTER PROGRAM

In making the computer calculations, values for the various operating conditions prevailing in Stage 1 and Stage 2 are first designated, together with an arbitrarily chosen Stage 1 product gas composition. Then, the heat of reaction is calculated for the reaction of recycle char with oxygen and steam in Stage 1 to form the Stage 1 product gas of the arbitrarily chosen composition. The heat of reaction is calculated from the heating value of the recycle char and of the Stage 1 product gas, and then used to calculate the Stage 1 gas exit temperature.

Assuming that the water-gas shift equilibrium is established at this temperature of Stage 1, a new gas composition is calculated next and then used to correct the gas temperature. This process is repeated until a Stage 1 exit gas temperature is found that has a calculated accuracy of ± 5 C.

The Stage 1 product gas is then used in Stage 2 where coal and steam are added and reacted to form CH_4 in a concentration corresponding to the equilibrium of Equation 1 at a designated carbon activity and at an estimated temperature. The carbon in the coal which is not used in making methane is reacted with steam to form CO and H_2 . Oxygen, nitrogen, and sulfur in the coal form H_2O , N_2 , and H_2S ; and the remaining hydrogen in the coal is liberated as gaseous hydrogen.

For this combination of gas from Stage 1 and Stage 2, again the temperature of the resultant gas mixture is calculated and the composition adjusted to reflect establishment of the shift reaction equilibrium. With the new composition, the equilibria for methane formation and the shift reaction are combined and the calculations reiterated until a Stage 2 temperature is obtained which is within ± 5 C of the actual temperature.

Computer Input

The nature of the input data required for the various individual computer calculations is shown in Table 1. The values for the different operating parameters were varied from one calculation to the next in accordance with the particular effect being evaluated.

TABLE 1. EXAMPLE OF COMPUTER INPUT DATA

<u>Item</u>	<u>Stage 1</u>	<u>Stage 2</u>	<u>Total</u>
Coal, daf, lb	--	100.0	100.0
Coal Preheat, C	--	204	--
Carbon Reacted, %	67	33	100.0
Carbon Activity, Equation 1	--	1.0	--
Oxygen, lb	71.0	--	71.0
Oxygen Preheat, C	327	--	--
Steam, lb	36.0	104.9	140.9
Steam Preheat, C	538	538	--
Pressure, atm	72.4	72.4	--
Heat Loss, Btu/lb Coal	250	--	250

Available data (7) for the heats of combustion, enthalpies, and thermodynamic equilibria were used in the computer program.

Computer Output

The type of information given in the printout for each computer run is shown in Table 2.

In addition to the results given in the computer output, some parameters indicative of the cost of the final gas, such as "total methane after methanation," "oxygen consumption lb/MM Btu in the final gas," or "the CO_2 production" have been manually calculated.

TABLE 2. EXAMPLE OF COMPUTER OUTPUT DATA

<u>Item</u>	<u>Stage 1, Moles</u>	<u>Stage 2, Moles</u>	<u>Stage 2, Mole Fraction</u>
Gas Composition			
CO	3.900	3.473	0.3138
H ₂ S	0.000	0.084	0.0076
CH ₄	0.000	1.165	0.1052
H ₂	1.036	3.900	0.3524
N ₂	0.000	0.057	0.0052
CO ₂	0.787	2.390	0.2159
Total	<u>5.723</u>	<u>11.069</u>	<u>1.0001</u>
H ₂ O	--	3.902	--
(CO + H ₂)	--	7.373	--
Temperatures, C	1715	935	--
Oxygen/Steam Ratio	1.972	--	--
Oxygen/Coal Ratio	--	0.710	--
Preformed Methane, %	--	38.722	--
C as Methane, %	--	16.575	--

COALS USED

Three coals varying in rank from high volatile A bituminous to lignite were used in the study to obtain an indication of the effect of coal composition. The analyses used for these coals are given in Table 3.

TABLE 3. COAL ANALYSES USED FOR COMPUTER STUDY

	<u>Seam</u>		
	<u>Pittsburgh</u>	<u>Illinois No. 6</u>	<u>Lignite</u>
H ₂ O, lb per 100 lb daf Coal	1.3	1.3	1.3
Ash, lb per 100 lb daf Coal	7.7	9.1	15.5
Ultimate Analyses, Percent daf			
C	84.4	81.3	74.3
H	5.7	5.4	4.8
N	1.6	1.5	0.9
O	5.6	9.6	18.5
S	2.7	2.6	1.5
Net H per 100 C	5.3	4.6	3.0
Gross Heating Value, Btu/lb	15,270	14,480	12,270

RESULTS AND DISCUSSION

The data from the thirteen runs using Pittsburgh seam coal in normal operation of the gasifier are summarized in Tables 4 and 5. These were Runs 27 through 37, 42, and 43. The data from the four runs with char withdrawal are summarized in Table 6; these were Runs 48, 49, 50, and 53, using Pittsburgh seam coal. Runs 38 and 39 using Illinois No. 6 seam coal, and Runs 51 and 52 using North Dakota lignite are summarized in Table 7.

The computer data were used to calculate parameters that can be used directly in comparing the costs of gases obtained with different computer input data or different operating conditions. These parameters are referred to one million Btu in the final gas after methanation, and are based on costs derived from the initial economic evaluation (1) as follows:

Coal:	15¢/MM Btu
Oxygen:	\$5/ton = 0.25¢/lb
CO ₂ Removal:	\$1/ton = 0.05¢/lb
Steam:	30¢/1000 lb

Oxygen/Coal Ratio and Temperature

For Pittsburgh seam coal, the influence of a change in the oxygen/coal ratio is shown in Figure 2, the oxygen/coal ratio is plotted versus Stage 2 temperature, oxygen consumption, CO₂ production, carbon as methane, and gasification efficiency. As expected, with increases in the oxygen/coal ratio, the Stage 2 temperature increases and all parameters connected with gasification cost indicate increased costs.

The data shown in Figure 2 are replotted in Figure 3 to show the effects of changes in Stage 2 temperature on these same parameters. Over the range studied, a Stage 2 temperature increase of 12 C causes a corresponding decrease in methane formation equal to about 1 percent of the carbon in the coal.

Carbon Activity

On the basis that experimental results may indicate a higher conversion to methane at a given temperature than indicated by Figures 2 and 3, adjustments were made in the computer calculations to reflect a higher activity for the carbon in Stage 2.

The results of computer runs using carbon activity 3.4 and 2, respectively, are compared in Table 8. The data show the influence of changes in methane yield from 14 to 24.6 percent on a carbon basis on the cost of the pipeline gas. A 1 percent unit increase in the conversion of the carbon in the coal into methane decreases the cost of raw materials and utilities for the pipeline gas by about 0.6¢/MM Btu.

In the initial evaluation of the processes (1), conversions of carbon into CH₄ in Stage 2 of 15, 20, and 24 percent were assumed; a 1 percent increase in the carbon conversion to methane decreased the pipeline gas cost by about 0.8¢/MM Btu.

Total Operating Pressure

In this study, the thermodynamic equilibrium is used to obtain the methane yield; therefore, the operating pressure exerts a major influence on the

TABLE 4. SUMMARY OF RESULTS OF COMPUTER RUNS 27-33

	Run Number 8014 BKC					
	27	28	29	30	32	33
<u>INPUT DATA</u>						
Type of Coal	Peb.	Peb.	Peb.	Peb.	Peb.	Peb.
System Pressure, atm	72.4	72.4	72.4	72.4	72.4	102.4
Input Temperature, °C	204	204	204	204	204	204
Coal	538	538	538	538	538	538
Steam	327	327	327	327	327	327
Oxygen						
<u>Stage 2</u>						
Coal Feed Rate, lb daf	100.0	100.0	100.0	100.0	100.0	100.0
Steam Feed Rate, lb	95.4	95.4	95.4	95.4	95.4	95.4
Carbon Activity	1.0	1.0	1.0	1.0	1.0	1.0
Carbon Reacted, %	33.3	33.3	33.3	29.9	24.7	33.3
<u>Stage 1</u>						
Steam Feed Rate, lb	36.0	36.0	36.0	36.0	36.0	36.0
Oxygen Feed Rate, lb	71.0	71.0	71.0	74.5	80.0	71.0
Heat Loss, Btu/lb Coal	250	250	0	250	250	250
<u>CALCULATIONS</u>						
<u>Stage 2</u>						
Temperature (Exit) °C	935	945	905	955	955	955
Temperature (Exit) °F	1715	1733	1661	1751	1805	1751
Gas Composition, Moles						
CO	3.473	4.990	3.180	3.662	3.616	3.374
H ₂ S	0.084	0.084	0.084	0.084	0.084	0.084
CH ₄	1.165	0.958	1.303	1.077	1.046	1.254
H ₂	3.900	3.209	3.639	4.064	4.013	3.643
N ₂	0.057	0.057	0.057	0.057	0.057	0.057
CO ₂	2.390	1.070	2.544	2.289	2.365	2.399
H ₂ O	3.902	1.043	3.886	3.915	4.027	3.981
<u>Stage 1</u>						
Temperature, °C	1715	1715	1575	1865	1735	1715
Temperature, °F	3119	3119	2867	3389	3155	3119
Gas, Moles						
CO	3.900	3.900	3.861	3.937	4.142	4.499
H ₂	1.036	1.036	1.075	0.999	1.054	1.036
CO ₂	0.787	0.787	0.886	0.749	0.784	0.787
H ₂ O	0.962	0.962	0.923	1.000	0.945	0.962
<u>Stage 2</u>						
Total Gas, Dry Moles	11.068	10.377	10.807	11.232	11.181	10.811
Total (CO + H ₂) Moles	7.373	8.198	8.819	7.725	7.629	7.017
Preformed CH ₄ , %	38.7	31.9	43.3	35.8	35.4	41.7
Carbon as Methane, %	16.6	13.6	18.5	15.3	14.9	17.8
<u>Total</u>						
Thermal Efficiency	0.836	0.864	0.825	0.842	0.828	0.830
Steam Decomposition, %	47	69	47	47	45	45
Moles, Total Methane after Methanation	3.01	3.01	3.01	2.95	2.86	3.01
% Btu in Coal, Total Methane after Methanation	75.5	75.5	75.5	74.0	71.7	75.5
Oxygen Consumption, lb/MM Btu in CH ₄	61.8	61.8	61.8	61.8	65.9	61.8
CO ₂ Production, Mole per Mole CH ₄	4.02	4.02	4.02	4.02	4.08	4.02
CO ₂ Production, lb/MM Btu in Gas	154	154	154	154	159	154

TABLE 5. SUMMARY OF RESULTS OF COMPUTER RUNS 34-37, 42, AND 43

	Run Number 8014, BKC-					
	34	35	36	37	42	43
INPUT DATA						
Type of Coal	Prh.	Prh.	Prh.	Prh.	Prh.	Prh.
System Pressure, atm	51.0	72.4	72.4	72.4	72.4	72.4
Input Temperature, °C						
Coal	204	204	204	204	204	204
Steam	538	538	538	538	538	538
Oxygen	327	327	327	327	327	327
Stage 2						
Coal Feed Rate, lb daf	100.0	100.0	100.0	100.0	100.0	100.0
Steam Feed Rate, lb	95.4	104.9	95.4	95.4	95.4	60.0
Carbon Activity	1.0	1.0	3.4	2.0	1.0	1.0
Carbon Reacted, %	33.3	33.3	39.8	39.8	39.8	33.3
Stage 1						
Steam Feed Rate, lb	36.0	36.0	36.0	36.0	36.0	36.0
Oxygen Feed Rate, lb	71.0	71.0	63.9	63.9	63.9	71.0
Heat Loss, Btu/lb Coal	250	250	250	250	250	250
CALCULATIONS						
Stage 2						
Temperature (Exit) °C	905	925	965	935	885	945
Temperature (Exit) °F	1661	1697	1769	1715	1625	1733
Gas Composition, Moles						
CO	3.476	3.256	2.792	2.961	3.045	4.137
H ₂ S	0.084	0.084	0.084	0.084	0.084	0.084
CH ₄	1.121	1.220	1.729	1.595	1.475	1.065
H ₂	4.070	3.895	2.768	3.134	3.529	3.636
N ₂	0.057	0.057	0.057	0.057	0.057	0.057
CO ₂	2.430	2.551	2.506	2.471	2.506	1.825
H ₂ O	3.819	4.326	3.906	3.807	3.652	2.401
Stage 1						
Temperature, °C	1715	1715	1665	1665	1665	1715
Temperature, °F	3119	3119	3029	3029	3029	3119
Gas, Moles						
CO	3.900	3.900	3.458	3.458	3.458	3.900
H ₂	1.036	1.036	1.009	1.009	1.036	1.036
CO ₂	0.787	0.787	0.773	0.773	0.773	0.787
H ₂ O	0.962	0.962	0.990	0.990	0.990	0.962
Stage 2						
Total Gas, Dry Moles	11.238	11.063	9.936	10.302	10.697	10.804
Total (CO + H ₂) Moles	7.546	7.152	5.560	6.095	6.575	7.772
Preformed CH ₄ , %	37.3	40.6	55.4	51.1	47.3	35.4
Carbon as Methane, %	16.0	17.4	28.6	22.7	21.0	15.2
Total						
Thermal Efficiency	0.838	0.830	0.832	0.840	0.847	0.848
Steam Decomposition, %	49	45	46	48	50	55
Moles, Total Methane after Methanation	3.01	3.01	3.12	3.12	3.12	3.01
% Btu in Coal, Total Methane after Methanation	75.5	75.5	78.3	78.3	78.3	75.5
Oxygen Consumption, lb/MM Btu in CH ₄	61.8	61.8	53.5	53.5	53.5	61.8
CO ₂ Production, Mole per Mole CH ₄	4.02	4.02	4.02	3.91	3.91	4.02
CO ₂ Production, lb/MM Btu in Gas	154	154	144	144	144	154

TABLE 6. SUMMARY OF RESULTS OF COMPUTER RUNS 48, 49, 50, AND 53

	Run Number 8014 BKC-			
	48	49	50	53
<u>INPUT DATA</u>				
Type of Coal	Pgh.	Pgh.	Pgh.	Pgh.
System Pressure, atm	72.4	72.4	72.4	72.4
Input Temperatures, °C				
Coal	204	204	204	204
Steam	538	538	538	538
Oxygen	327	327	327	327
<u>Stage 2</u>				
Coal Feed Rate, lb daf	100.0	100.0	100.0	100.0
Steam Feed Rate, lb	71.0	2.0	2.0	2.0
Carbon Activity	1.0	1.0	3.4	7.0
<u>Stage 1</u>				
Steam Feed Rate, lb	24.0	24.0	24.0	24.0
Oxygen Feed Rate, lb	65.0	28.0	20.0	20.0
Heat Loss, Btu/lb Coal	250	250	250	250
<u>CALCULATIONS</u>				
<u>Stage 2</u>				
Temperature (exit) °C	1035	945	915	945
Temperature (exit) °F	1895	1733	1679	1733
Gas Composition, Moles				
CO	3.178	0.954	0.526	0.452
H ₂ S	0.084	0.084	0.084	0.084
CH ₄	0.583	0.548	0.933	0.001
H ₂	3.567	1.668	0.971	0.774
N ₂	0.057	0.057	0.057	0.057
CO ₂	1.601	0.572	0.572	0.579
H ₂ O	3.378	1.518	1.445	1.506
<u>Stage 1</u>				
Temperature, °C	2355	995	725	725
Temperature, °F	4271	1823	1337	1337
Gas, Moles				
CO	1.737	1.551	1.129	1.129
H ₂	0.244	0.845	0.981	0.981
CO ₂	1.285	0.522	0.551	0.551
H ₂ O	1.088	0.488	0.351	0.351
<u>Stage 2</u>				
Total Gas, Dry Moles	9.070	3.882	3.143	2.946
Total (CO + H ₂) Moles	6.745	2.621	1.497	1.225
Preformed CH ₄ , %	25.7	45.5	71.4	76.6
Carbon as Methane, %	8.3	7.8	13.3	14.2
Char Produced, lbs C	20.0	60.0	60.0	60.0
<u>TOTAL</u>				
Thermal Efficiency	0.651	0.325	0.331	0.327
Steam Decomposition, %	36.1	-5.1	0.0	-4.0
Total Methane after Methanation				
Moles	2.27	1.202	1.306	1.306
% Btu in Coal	57.5	30.5	32.9	32.9
% Btu in (Coal minus Char)	70.2	69.2	75.0	75.0
Btu in Char as % of Btu in Coal	18.6	55.7	55.7	55.7
Btu in Gas and Char as % of Btu in Coal	76.1	86.2	88.6	88.6
Oxygen Consumption, lb MM Btu in CH ₄	75.5	60.5	40.0	40.0
CO ₂ Production, Mole/Mole CH ₄	1.36	0.73	0.56	0.56
CO ₂ Production, lb MM/MM Btu in Gas	156	83	64	64

TABLE 7. SUMMARY OF RESULTS OF COMPUTER RUNS 38, 39, 51, AND 52

INPUT DATA	Run Number 8014 BKC-			
	38	39	51	52
Type of Coal	Illinois	Illinois	Lignite	Lignite
System Pressure, atm	72.4	72.4	72.4	72.4
Input Temperatures, °C				
Coal	204	204	204	204
Steam	538	538	538	538
Oxygen	327	327	327	327
<u>Stage 2</u>				
Coal Feed Rate, lb daf	100.0	100.0	100.0	100.0
Steam Feed Rate, lb	95.4	95.4	55.0	95.4
Carbon Activity	1.0	1.0	1.0	1.0
Carbon Reacted, %	30.6	41.4	22.6	22.6
<u>Stage 1</u>				
Steam Feed Rate, lb	36.0	36.0	36.0	36.0
Oxygen Feed Rate, lb	71.0	60.0	65.0	65.0
Heat Loss, Btu/lb Coal	250	250	250	250
<u>CALCULATIONS</u>				
<u>Stage 2</u>				
Temperature (exit) °C	955	885	915	895
Temperature (exit) °F	1751	1625	1679	1643
Gas Composition, Moles				
CO	3.388	2.855	3.055	2.357
H ₂ S	0.081	0.081	0.047	0.047
CH ₄	0.975	1.391	0.910	1.038
H ₂	3.837	3.395	2.853	3.039
N ₂	0.054	0.054	0.032	0.032
CO ₂	2.405	2.522	2.220	2.790
H ₂ O	4.180	3.791	2.839	4.640
<u>Stage 1</u>				
Temperature, °C	1705	1635	1405	1405
Temperature, °F	3101	2975	2561	2561
Gas, Moles				
CO	3.906	3.196	4.184	4.184
H ₂	1.052	0.987	1.330	1.330
CO ₂	0.792	0.771	0.604	0.604
H ₂ O	0.947	1.011	0.669	0.669
<u>Stage 2</u>				
Total Gas, Dry Moles	10.741	10.299	9.118	9.304
Total (CO + H ₂) Moles	7.225	6.251	5.908	5.397
Preformed CH ₄ , %	35.1	47.1	38.1	43.5
Carbon as Methane, %	14.4	20.5	14.7	16.8
<u>Total</u>				
Thermal Efficiency	0.822	0.845	0.833	0.815
Steam Decomposition, %	43	48	44.0	36.6
Total Methane after Methanation, Moles	2.78	2.95	2.39	2.39
Total Methane after Methanation, % Btu in Coal	73.7	78.1	74.7	74.7
Oxygen Consumption, lb/MM Btu in CH ₄	66.5	53.2	71.0	71.0
CO ₂ Production, Mole per Mole CH ₄	3.99	3.82	1.59	1.59
CO ₂ Production, lb/MM Btu in Gas	165	148	183	183

TABLE 8. EFFECTS OF CHANGES IN CARBON ACTIVITY IN STAGE 2
(Basis: Pressure, 72.4 atm; Heat Loss, 250 Btu/lb Coal)

	Stage 2 Temperature, 935 C			Stage 2 Temperature, 965 C		
	Carbon Activity 2.0	Carbon Activity 1.0	Difference φ/MM Btu in Gas	Carbon Activity 3.4	Carbon Activity 1.0	Difference φ/MM Btu in Gas
Oxygen, lb/100 lb Coal	63.9	71.0	--	63.9	75.9	--
Carbon as CH ₄ , %	22.7	16.6	--	24.6	14.0	--
Gasification Efficiency, %	78.3	75.5	--	78.3	73.2	--
Oxygen, lb/MM Btu in Gas	53.5	61.8	8.3	53.5	68.1	14.6
CO ₂ , lb/MM Btu in Gas	144.0	154.0	10.0	144.0	163.0	19.0
Steam, lb/MM Btu in Gas	110.0	114.5	4.5	110.0	118.0	8.0
Coal, MM Btu/MM Btu in Gas	1.277	1.325	0.048	1.277	1.367	0.09
TOTAL			3.42			6.19

8008G193

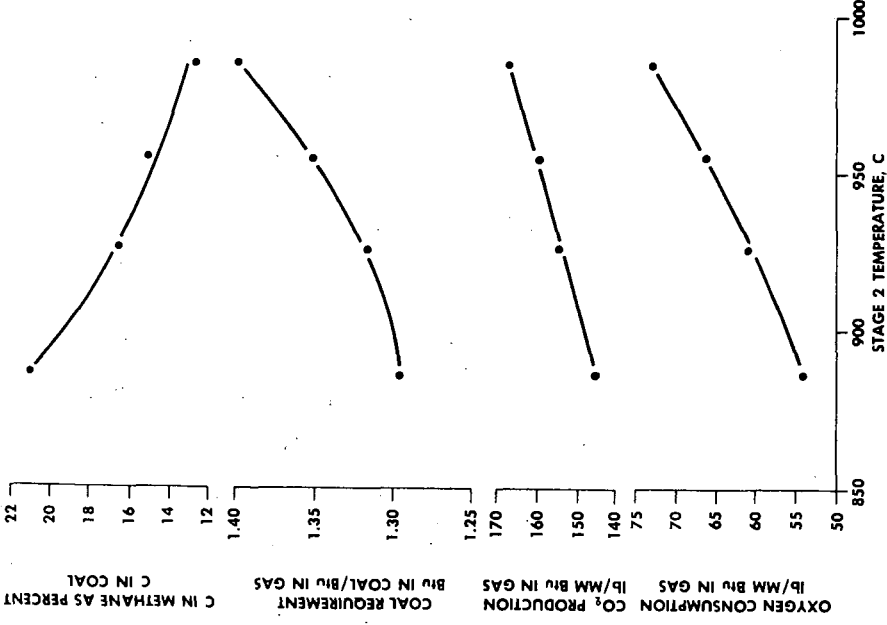


Figure 3. Effects of Changes in Stage 2 Temperature (Basis: Pressure, 72.4 atm, Heat Loss: 250 Btu/lb Coal)

8008G113

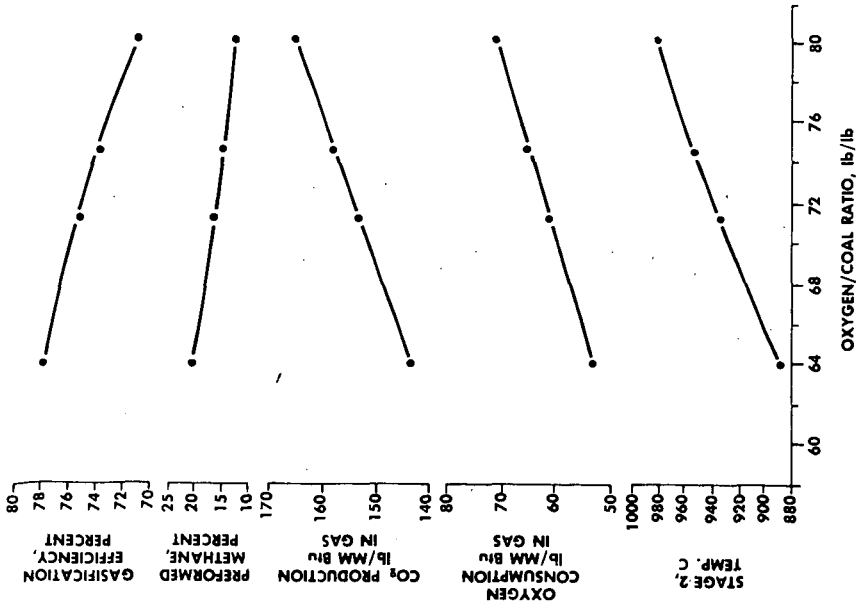


Figure 2. Computer Program Results: Effects of Changes in Oxygen (Basis: Pressure, 72.4 atm, Heat Loss: 250 Btu/lb Coal)

yield. By comparing the results from Run 33 and Run 34 with those from a run at the standard operating pressure, it is noted that a change in pressure, either from 72.5 to 51 atm, or from 72.5 to 102 atm, produces a change in raw material and utility costs equivalent to about 2¢/MM Btu pipeline gas; operation at the higher pressure gives the cheaper gas in each case. By comparison, the same change in gas cost of 2¢/MM Btu would be produced by a change of about \$10 million in the investment costs for a 250 MM scfd plant. Further economic evaluations and experimental results will be needed to find the optimum pressure for the lowest cost of gas and/or capital investment.

Heat Loss and Preheat Temperature

Another factor influencing the gas yield is the heat loss in the gasifier. As reference value, a heat loss of 250 Btu/lb of coal, or 1.6 percent of the heating value of Pittsburgh seam coal, has been assumed. This is an arbitrarily chosen figure that is based on extrapolation of available data to pressure operation. Computer Runs 29 and 30 for heat losses of 500 and 0 Btu/lb of coal, respectively, were compared with results for 250 Btu heat loss at the same Stage 2 temperature. An increase in heat loss of 250 Btu/lb coal increases the gas cost by about 2¢/MM Btu pipeline gas. Again, experimental studies will be needed to determine whether the actual methane yield is influenced to the extent indicated here. Only experiments in a large pilot plant will establish reliable data for the heat loss in a commercial unit.

A study of different preheat temperatures of reactants did not appear necessary. Differences in the enthalpies of the various materials due to changes in preheat temperature, have the same influence as changes in heat loss.

Steam/Coal Ratio

Several computer runs were made using various steam/coal ratios:

In Computer Runs 28 and 35, data for 24.0 and 104.9 pound steam per 100 pound coal in Stage 2 were obtained for comparison to the "standard" quantity of 95.4 pound; no changes were made in the amount of steam entering Stage 1, 36.0 pound steam per pound coal being used in all instances.

In Computer Run 28 with 60 pound total steam per 100 pound coal, the Stage 2 temperature was 20 C above that in Run 35, being 945 C, as compared to 925 C.

Unless reaction kinetics demand a high steam/coal ratio, a ratio below 130 lb/100 lb coal should be selected for purely heat balance reasons. A further study of the utilization of the gasification steam in the shift reactor is indicated. Such a reactor would be part of an integrated pipeline gas plant.

Withdrawal of Recycle Char

On the premise that it may become desirable to withdraw recycle char for use as boiler fuel rather than fresh coal, Computer Runs 48, 49, 50, and 53 were made to indicate results which might be expected with such an operation. The partial gasification shows lower costs for pipeline gas in all cases: the lowest difference is 2.4 cents, the highest 13.3 cents per MM Btu based on raw material and utility costs only, assuming a char credit at the Btu price of the coal and only a minor char handling expense.

Additional experimental data are needed to better define the methane yield and operating temperature for char withdrawal in comparison to these same parameters for complete gasification.

Changes in Coal Feed Stock

To obtain data on the effect of coal rank on the cost of pipeline gas, several computer runs were made with coals differing in rank from Pittsburgh seam coal, namely, Runs 38 and 39 with Illinois No. 6 coal and Runs 51 and 52 with lignite. For Pittsburgh seam coal and Illinois No. 6 coal at the same price per MM Btu in the dried coal and the same Stage 2 temperature, the pipeline gas cost is similar. On the same basis, the greater thermal ballast in the lignite, mainly its high oxygen content, leads to a higher cost of gas made from lignite. However, if one assumes a 60 C lower Stage 2 temperature for lignite, the gas cost becomes the same.

Again, further experimentation will lead to a better definition of the best operating temperature for the various coals and a better comparison of cost will be possible.

Comparison of Experimental and Computer Results

Experimental Stage 2 gasification data for lignite (3) are compared with computer results in Table 9. The experimental results show a somewhat higher methane yield in spite of higher Stage 2 temperatures. This discrepancy is not surprising since the methane yield is determined by reaction kinetics and factors such as partial pressures of reactants and the ratios of Stage 1 gas, steam, and coal, rather than by the thermodynamic equilibria.

The higher experimental yield of ($\text{CO} + \text{CO}_2$) will lead to a smaller amount of char available for Stage 1 than used in the computer run. This will, at the same oxygen/coal ratio, lead to a higher Stage 1 temperature. To attain the higher temperature in Stage 2 indicated by the experiments, a higher oxygen/lignite ratio than the 0.65 lb/lb assumed in computer Run 51 will be needed. In the feed streams entering Stage 2 in the experimental runs, the partial pressure of ($\text{CO} + \text{H}_2$) is lower; and that of CO_2 is higher than in the computer run. This is in accord with a higher oxygen/lignite ratio as required to attain the higher temperature used in the experimental runs. It may be noted that the Stage 1 gas/lignite ratios and the steam/lignite ratios in the two experimental runs bracket these same parameters in the computer runs.

The computer data reported in this study have been useful in providing guidance for the selection of experimental parameters such as feed stream composition and reactant ratios for the externally-heated experimental 5 lb/hr flow reactor being used for the study of Stage 2 reactions. They will be equally useful in the operation of the internally-heated 100 lb/hr process and equipment development unit now being erected.

The computer program used in this study may also be useful as a basis in preparing an improved program in which the methane content of the Stage 2 gas is determined by kinetic data. It is expected that further operation of the 5 lb/hr unit, and later the 100 lb/hr unit, will supply such data.

TABLE 9. EXPERIMENTAL AND COMPUTER DATA FOR
LIGNITE GASIFICATION IN STAGE 2

	<u>Experimental Data</u>		<u>Computer Data</u>
	<u>Run 36</u>	<u>Run 38</u>	<u>Run 51</u>
Temperature °C, Stage 1	--	--	1405
Stage 2	970	965	915
Pressure, atm	70	81.5	72.4
Lignite, g C/min	5.9	18.8	--
Stage 1 Gas, ml/g C in Lignite	4.9	1.56	1.84
Steam, g/g C in Lignite	2.1	0.9	1.22
Partial Pressure of Gases Entering Stage 2, atm			
CO	25.5	26.5	30.8
H ₂	8.4	8.7	9.8
CO ₂	7.5	7.9	4.4
H ₂ O	24.5	34.0	27.4
Ar	4.1	4.4	--
Yields in Stage 2 alone as Percent of Lignite:			
C in CH ₄	16.9	15.4	14.7
C in (CO + CO ₂)	<u>22.0</u>	<u>18.1</u>	<u>7.9</u>
C Gasified in Stage 2	38.9	33.5	22.6
Btu in CH ₄	33.8	29.5	28.2
Btu in (CO + H ₂)	4.5	10.2	3.8

ACKNOWLEDGMENT

This paper reports results from a program of research being conducted by Bituminous Coal Research, Inc., with support from the Office of Coal Research, U.S. Department of the Interior, under Contract No. 14-01-0001-324. The authors wish to thank the Office of Coal Research for permission to publish this paper.

The authors also wish to express their thanks to Mr. E. J. Vidt and the Blaw-Knox Company for preparing the computer program and making the computations.

REFERENCES

1. "Gas Generator Research and Development - Survey and Evaluation," (Bituminous Coal Research, Inc., Report L-156), Two Volumes, 650 pp, Washington, D.C.: U.S. Government Printing Office, 1965.
2. Donath, E. E. and Glenn, R. A., "Pipeline gas from coal by two-stage entrained gasification," Proc. AGA Production Conference, 1965, 65-P-147 to 65-P-151 (1965).
3. Glenn, R. A., Donath, E. E., and Grace, R. J., "Gasification of coal under conditions simulating stage 2 of the BCR two-stage super-pressure gasifier," Am. Chem. Soc., Div. Fuel Chem. Preprints 10 (4), 97-122 (1966).
4. Glenn, R. A. and Grace, R. J., "Laboratory-scale flow reactor for studying gasification of coal under conditions simulating stage 2 of the BCR two-stage super-pressure gasifier," Presented at North-Central Regional AIChE Symp. on Current Trends in Pilot Plants, Pittsburgh, Pa., 1967.
5. Peters, W., "Schnellentgasung von Steinkohlen," Thesis, Aachen, 1963; Peters, W. and Bertling, H., "Kinetics of the rapid degasification of coals," Fuel 44, 317-31 (1965).
6. Squires, A. M., "Steam-oxygen gasification of fine sizes of coal in a fluidised bed at elevated pressure," Trans. Inst. Chem. Engrs. (London) 39 (1), 3-22 (1961).
7. Wagman, D. D., et al, "Heats, free energies, and equilibrium constants of some reactions involving O₂, H₂, H₂O, C, CO, CO₂, and CH₄," U.S. Dept. Commerce, Natl. Bur. Std., Res. Rept. 1634 (1945).

CATALYTIC DEHYDROGENATION OF COAL III. HYDROGEN EVOLUTION AS A FUNCTION OF RANK*

R. Raymond, L. Reggel, and I. Wender

Pittsburgh Coal Research Center, U. S. Bureau of Mines,
4800 Forbes Avenue, Pittsburgh, Pa. 15213

Dehydrogenation of coal using a one percent palladium on calcium carbonate catalyst in the presence of phenanthridine as solvent gives almost pure hydrogen gas as the product. The rank of coal affects the yield of hydrogen from the corresponding vitrain; for coals ranging from high volatile C bituminous to anthracite, the hydrogen evolution decreases gradually with increasing rank of coal; lignites and subbituminous coals give less hydrogen than do low rank bituminous coals. For bituminous coals, the hydrogen evolution (atoms of hydrogen evolved per 100 carbon atoms in the coal) is a linear function of the atomic H/C ratio and also of the atomic O/C ratio. Lignites and subbituminous coals fall outside of the lines defining the bituminous coals. Some ideas on the process of coalification are presented: it is suggested that lignites and subbituminous coals contain some cyclic carbon structures which are neither aromatic nor hydroaromatic; that low rank bituminous coals contain large amounts of hydroaromatic structures; and that higher rank bituminous coals contain increasing amounts of aromatic structures.

INTRODUCTION

The vast literature on chemical reactions of coal^{1,2} contains (until quite recently) very few references to any work on dehydrogenation. This may be due in part to the paucity of systematic studies on the dehydrogenation of organic compounds under conditions which might be expected to cause relatively little disruption of the coal structure; i.e., dehydrogenation in the liquid phase[†] at temperatures below 400°C. The dehydrogenation reagents usually used for pure compounds are metallic catalysts³, sulfur³, selenium³, and quinones^{3,4}. The dehydrogenation of coal by sulfur⁵ has received considerable attention; the hydrogen removed from the coal is evolved as hydrogen sulfide. Selenium has not, to our knowledge, been used with coal; because of the higher temperature required and the poor yields usually obtained, selenium seldom offers any advantage over sulfur³; in a selenium dehydrogenation, the hydrogen removed is evolved as hydrogen selenide. Benzoquinone with coal has been investigated⁶; the reaction is a hydrogen transfer⁴, giving hydroquinone, and the results are difficult to interpret⁷. Iodine as a dehydrogenation agent has also been studied with coal⁸; the hydrogen removed from the coal is evolved as hydrogen iodide. Again, the results are not easy to evaluate; the temperature of reaction is high; and there is very little work on organic compounds which can serve as a basis for comparison^{9,10}. Bromine, one of the oldest dehydrogenation reagents³, has been of little value¹.

The first use of a metallic catalyst for the dehydrogenation of coal was reported by the present authors¹¹; the reaction was conducted in the presence of a solvent (vehicle), and almost pure hydrogen gas was evolved. The reversibility of the reduction and dehydrogenation of coal has also been investigated¹². In this paper we wish to summarize the development of the method, the experimental

*For the preceding papers in this series, see references 11 and 12.

† For an excellent and up to date review see ref. 3.

procedure, and, most important, the effect of the rank of the coal upon the amount of hydrogen formed. The purpose of these studies is twofold: first, to obtain information which may give some insight into the structure of coal; second, to obtain large amounts of hydrogen from coal. It is hoped that development of cheaper solvents and catalysts might enable hydrogen to be produced economically; the coal residue could then be burned for fuel.

EXPERIMENTAL

Preliminary experiments in which coal, catalyst, and vehicle were refluxed showed that the hydrogen evolution was influenced by reflux rate, heating rate, bath temperature, and depth of immersion of the reaction flask into the bath. Accordingly, the previous apparatus used a stirrer and a heating mantle^{11,12}. A Hershberg tantalum wire stirrer with a glass bearing lubricated with silicone grease was used; later, a magnetic stirrer was found to be more convenient, to give superior results, and to obviate crust problems (see below). When the Hershberg stirrer was used, the reactants (0.500 g of dried, -200 mesh coal, 0.550 g of catalyst, and 7.50 g of the vehicle) were weighed into a 50 ml two-neck flask. The charge was mixed thoroughly with a spatula. The flask was then fitted with the stirrer and with an adapter which included both a dip-tube to serve as a thermocouple well and a side arm which was attached to a 250 ml gas buret. Provision was made for admission of helium to the system and for sampling the evolved gas after the reaction. The apparatus was thoroughly flushed with helium and pressure-tested for leaks. Flushing consisted essentially of admitting helium to the system, expelling the gas, adding fresh helium, and repeating this procedure three to five times. As a check upon the efficacy of flushing, the last expelled flush can be sampled; it should contain at least 99 percent helium (all gases were analyzed by mass spectrometry). The charge was then vigorously refluxed (heating mantle) with stirring for 5.0 h, preceded by a carefully standardized 0.5-h period of heating up to temperature. The reduced 1 percent palladium on calcium carbonate catalyst was prepared by Engelhard Industries, Inc., Newark, N. J. The same batch of catalyst was used in all of the runs described here, with the exceptions noted below. (See Discussion.) The catalyst was dried at 60°C and 1 mm; coals were dried to constant weight at 100° and 1 mm.

This experimental procedure was effective, but it was not convenient, and the stirrer sometimes jammed in the bearing, requiring repetition of a run. Also, some catalysts were found to convert the coal to a hard, brittle, insoluble crust after only a short heating period; this gave low and erratic values for hydrogen. (Crust formation could sometimes be avoided by very slow and prolonged heating to reflux.) It was found that magnetic stirring circumvented these problems and was also much more convenient. A 35 ml one-neck flask heated by an electric mantle was used. A pyrex-enclosed alnico stirring bar, 7/8 in. long, was placed in the flask. An alnico horseshoe magnet (ca. 50 pound pull) was located below the mantle and rotated by an ordinary stirring motor. The rest of the apparatus was as described above. With this modification, stirring was much more vigorous and crust formation usually did not take place. If in any run a solid crust began to form on the surface of the boiling liquid or on the walls of the flask, stirring was stopped and a small alnico magnet was brought near a point on the side of the flask; this pulled the stirring bar away from the large magnet, and the bar was moved around to break the crust. The small magnet was then removed, and stirring resumed with the large magnet. A few repetitions of this broke up any crust.

For most coals, the bulk of the gas was evolved during the first two hours of reflux, but gas evolution was still continuing at a slow rate (ca. 4 or 5 ml in 30 min) after 5 h. At the end of the reaction period, the gas volume was measured and the gas then thoroughly mixed and sampled. A typical analysis (helium-free basis) for the gas from an hvab coal is 96.4 percent H₂, 0.5 percent N₂, 0.4 percent CH₄, 0.1 percent ethylene, 0.6 percent CO, 0.1 percent ethane, 1.5 percent CO₂, and small amounts (0.1 percent) of other alkanes and alkenes. Lower rank coals gave larger amounts of CO, CO₂, and CH₄. Only the molecular hydrogen itself was considered to be hydrogen evolved; hydrogen in hydrocarbons was disregarded. In the calculations, it was assumed that the gas was saturated with water vapor. In all instances, blank runs (vehicle and catalyst, no coal) were made and corrections applied. The blanks were found to be a function of both the vehicle and the catalyst; two different batches of the same catalyst would give slightly different blanks. Coal-vehicle blanks (without catalyst) were found to be negligible and were disregarded. As would be expected, inadequate flushing of the apparatus led to low hydrogen values. It was also found that slight air oxidation of vitrains resulted in low hydrogen values; it is desirable to use a sample within a period of two weeks of grinding.

We thank D. E. Wolfson for obtaining many of the coal samples used. We are very grateful to B. C. Parks, Pittsburgh Mining Research Center, Bureau of Mines, who prepared the hand picked vitrain samples.

DISCUSSION

In the preliminary development of the method, some experiments were done on the dehydrogenation of 1,2,3,4,5,6,7,8-octahydrophenanthrene, using a 5 percent rhodium on alumina catalyst and refluxing *o*-terphenyl (bp 332°C) as a vehicle. No stirring was used. With a bath temperature of 300°-350°C for 1 h, about 98-99 percent of the theoretical amount of hydrogen gas was obtained, but the hydrogen evolution was never quite 100 percent. No formation of triphenylene (by cyclo-dehydrogenation of *o*-terphenyl) could be detected. In one experiment octahydrophenanthrene was dehydrogenated in the presence of about 5 percent by weight of dibenzothiophene (no vehicle); the hydrogen evolution was high (in addition, some hydrogen probably was used to cleave carbon-sulfur bonds) and the yield of phenanthrene was over 95 percent. It is thus apparent that the sulfur in coal should not poison the dehydrogenation catalyst. This is in accord with several reports on the dehydrogenation of partially reduced heterocyclic sulfur¹⁰, oxygen¹³, and nitrogen¹⁴⁻¹⁷ compounds, in good yield, with little cleavage of the carbon-hetero atom bond; for example, 1,2,3,4-tetrahydrodibenzothiophene is converted to dibenzothiophene by palladium on carbon in 80 to 94 percent yield¹⁰.

Experiments were then done on dehydrogenation of vitrain from Bruceton coal (hvab, Pittsburgh Bed, Bruceton, Allegheny County, Pa.) with various catalysts. Vitrain refluxed (without stirring) 2 h with *o*-terphenyl and 30 percent palladium on calcium carbonate gave off about 7.3 percent of the hydrogen in the vitrain as hydrogen gas; a pyridine-soluble extract of Bruceton vitrain under the same conditions gave 9.0 percent of its hydrogen; the pyridine soluble extract with phenanthridine as vehicle and 30 percent palladium on calcium carbonate gave 13.7 percent hydrogen in 2 h reflux and 30 percent hydrogen in 7 h. Bruceton vitrain with 30 percent palladium on carbon heated at 377° to 402°C (no vehicle) gave 0.2 percent hydrogen. Bruceton vitrain refluxed with *o*-terphenyl and various palladium, ruthenium, and rhodium catalysts gave 3 to 7 percent hydrogen. Bruceton vitrain refluxed 2 h with *o*-terphenyl and a molybdenum sulfide or tungsten sulfide catalyst gave both hydrogen (about 2 percent) and hydrogen sulfide; these results did not seem promising and no further work was done with sulfide catalysts.

All of the experiments discussed above were done with a refluxing system but no stirrer. Attention then turned to the development of an apparatus which could be stirred. Our previously published work^{11,12} was done using the Hershberg stirrer. The remainder of the work discussed in this paper used the magnetic stirrer (see Experimental), and is concerned with the effect of the rank of the coal upon the hydrogen evolved from the corresponding vitrain. It should be pointed out that comparison of the present results with previous data showed that, for most vitrains, magnetic stirring gave significantly greater yields of hydrogen than did the Hershberg stirrer. It seems probable that even with those vitrains and catalysts which have little tendency to form crusts with the Hershberg stirrer, an insolubilization reaction (polymerization, cross-linking, etc.) takes place during dehydrogenation which results in the coal being made too insoluble in the vehicle to react further, after partial but not complete dehydrogenation. With the more efficient magnetic stirring, dehydrogenation goes at a more rapid rate and is completed before insolubilization can have much effect on the final hydrogen evolution. Some data substantiating this is given in table 4, which shows that for two representative vitrains (Harmattan and Pocahontas No. 3), which give more hydrogen with magnetic than with Hershberg stirring, the magnetically stirred run evolves gas at a faster rate. However, for Bruceton vitrain (the only vitrain giving essentially the same hydrogen value for both stirring methods) the rates of gas evolution are almost the same for both runs.

Table 1 gives the identity and source of 36 coals used in this work. Of these, cannel coal was taken with the thought that its high hydrogen content might lead to a large hydrogen evolution, a hope which did not materialize. Cannel coal was used as the whole coal. The two semianthracites were also whole coals; microscopic examination showed that the Western Middle Field contained over 90 percent vitrain; the Bernice Field was less than 25 percent vitrain. The other 33 coals were used in the form of hand-picked vitrains. Tables 2 and 3 give the ultimate analyses of the samples and the results of dehydrogenation. The results are expressed in three ways: percent of the total hydrogen in the coal which is evolved as hydrogen gas; atoms of hydrogen evolved per 100 carbon atoms in the starting material; and milliliters of hydrogen evolved per gram of starting material.* The last figure (ml/g) can be converted to cubic feet per ton by multiplying by 32.0. This would obviously be of interest in indicating in a very rough way the possible economic value of the process. The largest value obtained is for the vitrain from a Utah hvcb coal (Liberty mine) which gives 9380 cubic feet of H₂ gas per ton on a dry basis, or 9890 cubic feet per ton on a dry ash-free basis. The second figure (H/100 C atoms) is related to the hydroaromatic† structures in the starting coal (neglecting side reactions for the present); any completely reduced structure such as cyclohexane, decalin, or perhydrocoronene would give a value of 100 H/100 C. The first figure (percent H₂ evolved) is also related to the amount of hydroaromatic structure in the coal, but not in a simple and direct manner; it is, however, a convenient figure in that it expresses a yield of product.

*The first two of these are independent of ash content; the third is not, and is on an ash basis.

†The term hydroaromatic is used in the sense defined by Fieser and Fieser¹⁸. Hydro derivatives of aromatic compounds are called hydroaromatic. Alicyclic substances containing six-membered rings but having substituents that block conversion to the aromatic state unless they are eliminated (such as 1,1-dimethylcyclohexane or 9-methyldecalin) are not classified as hydroaromatic.

Table 1. Identity and source of samples used in dehydrogenation

Lignite, Beulah-Zap Bed, Zap Mine, North American Coal Co., Zap, Mercer County, North Dakota

Lignite, Kincade Mine, Burke County, North Dakota

Lignite, Beulah-Zap Bed, North Unit, Beulah Mine, Knife River Coal Mining Co., Beulah, Mercer County, North Dakota

Subbituminous, Roland-Smith Bed, Wyodak Strip Mine, Wyodak Coal and Manufacturing Co., Gillette, Campbell County, Wyoming

Subbituminous, Dietz Bed, Big Horn Mine, Sheridan County, Wyoming

Subbituminous, Laramie Seam, Washington Mine, Clayton Coal Co., Erie, Weld County, Colorado

Subbituminous, Pioneer Canon No. 1 Mine, W. D. Corley Co., Florence, Fremont County, Colorado

Subbituminous, Rock Springs No. 7, 7-1/2, 9, and 15 Coal Beds, Superior, Sweetwater County, Wyoming

High-volatile B bituminous, Illinois No. 6, Green Diamond Mine, Mid-Continent Coal Corp., Marissa, St. Clair County, Illinois

High-volatile B bituminous, Illinois No. 6 Seam, Mecco Mine, Atkinson, Henry County, Illinois

High-volatile C bituminous, No. 11 Coal Bed, Rainbow No. 7 Mine, Gunn-Quealy Coal Co., Quealy, Sweetwater County, Wyoming

High-volatile C bituminous, Illinois No. 7 Bed, Harmatten Mine, Vermillion County, Illinois

High-volatile C bituminous (possibly high-volatile B bituminous), Liberty Bed, Liberty Mine, Liberty Fuel Co., Helper, Carbon County, Utah

High-volatile B bituminous, Illinois No. 6 Bed, Orient No. 3 Mine, Freaman Coal Mining Corp., Waltonville, Jefferson County, Illinois

High-volatile B bituminous, Kentucky No. 9, Pleasant View Mines 9-11, Western Kentucky Coal Co., Madisonville, Hopkins County, Kentucky

High-volatile B bituminous, Kentucky No. 9, DeKoven Mine, Sturgis, Union County, Kentucky

High-volatile A bituminous, Pittsburgh Bed, Bruceton, Allegheny County, Pennsylvania

High-volatile A bituminous, Pond Creek Coal, Majestic Mine, Pike County, Kentucky

High-volatile A bituminous, Powellton Bed, Elk Creek No. 1 Mine, Logan County, West Virginia

High-volatile A bituminous, Eagle Bed, Kopperston Mine, Kopperston, Wyoming County, West Virginia

Medium-volatile bituminous, Sewell Bed, Lochgelley Mine, New River Coal Co., Lochgelley, Mt. Hope, Fayette County, West Virginia

Medium-volatile bituminous (possibly high-volatile A bituminous), Lower Freeport Bed, Coal Valley No. 7 Mine, Indiana County, Pennsylvania

Low-volatile bituminous, Lower Kittanning Bed, Melcroft Mine, Eastern Associated Coal Corp., Fayette County, Pennsylvania

Medium-volatile bituminous, Lower Banner, Buccaneer Mine, Patterson, Buchanan County, Virginia

Medium-volatile bituminous, Sewell Bed, Marianna Mine, Wyoming County, West Virginia

Low-volatile bituminous, Beckley Bed, Maben Mine, Raleigh County, West Virginia

Medium-volatile bituminous, Sewell Seam, Crab Orchard Mine, Winding Gulf Coals, Inc., Raleigh County, West Virginia

Low-volatile bituminous, Lower Hartshorne Bed, Garland Coal and Mining Co., Prospect opening, Arkoma Coal Basin, Le Flore County, Oklahoma

(Continued)

Low-volatile bituminous, Upper Kittanning Bed, Stineman No. 10 Mine, Johnstown, Cambria County, Pennsylvania
 Low-volatile bituminous, Pocahontas No. 4 Bed, McAlpine Mine, Winding Gulf Coals, Inc., McAlpine, Raleigh County, West Virginia
 Low-volatile bituminous, Lower Kittanning Bed, Toth Mine, Hooversville, Cambria County, Pennsylvania
 Low-volatile bituminous, Pocahontas No. 3 Bed, Buckeye No. 3 Mine, Page Coal and Coke Co., Stephenson, Wyoming County, West Virginia
 Semianthracite, Bernice Field, Buckwheat No. 1 Mine, E and B Coal Co., Mildred, Sullivan County, Pennsylvania
 Semianthracite, Western Middle Field, Buckwheat No. 5 Mine, Trevorton Anthracite Co., Trevorton, Northumberland County, Pennsylvania
 Anthracite, Dorrance Mine, Lehigh Valley Coal Co., Luzerne County, Pennsylvania
 Cannel coal, Mine 27, Island Creek Coal Co., Logan County, West Virginia

Table 4. Evolution of gas from vitrains during the dehydrogenation process

Run No.	Vitrain	Stirring	Gross gas evolved, ml ^a				
			1 h	1.5 h	2 h	2.5 h	5.5 h
8R-61	Harmatten	Hershberg	62	84	100	111	155
8R-184	Harmatten	Magnetic	66	104	122	134	172
8R-109	Bruceton	Hershberg	51	77	92	104	147
8R-172	Bruceton	Magnetic	60	85	95	111	148
7R-167	Pocahontas No. 3	Hershberg	26	33	38	41	60
8R-182	Pocahontas No. 3	Magnetic	37	48	55	61	83

^a Approximate value for total gas evolved by the sample at the end of the indicated time, corrected to room conditions (ca. 25°C and 740 mm Hg pressure). The time given is from the beginning of the run; since the reaction mixture takes about one-half hour to reach operating temperature, the actual reaction time is about 0.5 h less than the time given. No correction for gas composition has been made.

Table 2. Analyses (moisture-free basis) of vitrains used for dehydrogenation

Run No.	Vitrain	C	H	N	S	Ash	O (by difference)	C, maf
9R-32	Beulah-Zap (Zap Mine)	64.18	5.28	0.85	0.58	5.35	23.76	67.81
8R-190	Kincade	64.96	4.59	.61	.55	4.73	24.56	68.19
9R-40	Beulah-Zap (Beulah Mine)	66.45	5.40	.31	1.40	3.60	22.84	68.93
9R-42	Roland-Smith (Wyodak)	62.76	5.35	1.01	1.14	10.58	19.16	70.19
9R-3	Dietz (Big Horn)	68.55	4.90	.99	.57	3.23	21.76	70.84
9R-134	Laramie (Washington)	68.11	5.30	1.57	.45	4.80	19.77	71.54
9R-132	Pioneer Canon No. 1	68.75	5.07	.90	1.25	5.23	18.80	72.54
8R-156	Rock Springs	73.21	5.17	1.38	.80	.66	18.78	73.70
8R-161	Illinois No. 6 (Green Diamond)	74.30	5.56	1.13	2.52	1.79	14.70	75.65
8R-162	Illinois No. 6 (Mecco)	74.71	5.39	1.03	2.05	1.77	15.05	76.06
9R-34	No. 11 (Rainbow No. 7)	75.54	5.63	1.92	.84	1.28	14.79	76.52
8R-184	Illinois No. 7 (Harmatten)	75.79	5.29	1.31	1.76	1.03	14.82	76.58
9R-41	Liberty	73.72	5.85	1.65	.72	5.06	13.00	77.65
8R-186	Illinois No. 6 (Orient No. 3)	77.64	5.16	1.87	1.14	1.89	12.30	79.14
8R-159	Kentucky No. 9 (Pleasant View)	78.12	5.89	1.58	1.97	1.54	10.90	79.34
8R-158	Kentucky No. 9 (DeKoven)	78.59	5.81	1.30	2.04	2.61	9.65	80.69
8R-143	Pittsburgh (Bruceton)	81.72	5.50	1.27	1.30	1.65	8.56	83.09
8R-172	Pittsburgh (Bruceton)	81.72	5.50	1.27	1.30	1.65	8.56	83.09
8R-147	Pittsburgh (Bruceton)	81.72	5.50	1.27	1.30	1.65	8.56	83.09
8R-149	Pittsburgh (Bruceton)	81.72	5.50	1.27	1.30	1.65	8.56	83.09
8R-160	Pond Creek (Majestic)	82.41	5.48	1.34	.81	1.59	8.37	83.74
8R-187	Powellton (Elk Creek No. 1)	84.46	5.28	1.53	.96	.69	7.08	85.05
8R-157	Eagle (Kopperston)	84.44	5.52	1.45	.97	2.03	5.59	86.19
8R-165	Sewell (Lochgelley)	85.74	5.20	1.44	.79	.79	6.04	86.42
8R-176	Lower Freeport (Coal Valley No. 7)	85.17	5.13	1.42	1.15	2.42	4.71	87.28
8R-175	Lower Kittanning (Melcroft)	85.34	5.00	1.51	1.46	2.32	4.37	87.37
8R-167	Lower Banner (Buccaneer)	85.37	5.23	1.29	.71	3.42	3.98	88.39

(Continued)

Run No.	Vitrain	C	H	N	S	Ash	O (by difference)	C, maf
8R-164	Sewell (Marianna)	88.15	5.00	1.43	.77	.88	3.77	88.93
8R-174	Beckley (Maben)	87.79	4.70	1.60	1.12	1.29	3.50	88.94
8R-166	Sewell (Crab (Orchard)	87.79	4.99	1.36	.59	1.68	3.59	89.29
9R-133	Lower Hartshorne	86.06	4.80	1.70	.73	3.87	2.84	89.52
8R-185	Upper Kittanning (Stineman No. 10)	87.64	4.84	1.44	.87	2.70	2.51	90.07
8R-181	Pocahontas No. 4 (McAlpine)	89.23	4.59	1.49	.81	1.15	2.73	90.27
8R-183	Lower Kittanning (Toth)	88.35	4.82	1.32	.74	2.34	2.43	90.47
8R-182	Pocahontas No. 3 (Buckeye No. 3)	89.57	4.67	1.25	.81	1.53	2.17	90.96
9R-119	Semianthracite (Bernice) ^a	79.22	3.43	1.01	.65	11.97	3.72	89.99
9R-118	Semianthracite (Western Middle) ^b	77.55	3.42	1.25	.85	14.36	2.57	90.55
8R-189	Dorrance anthracite	91.06	2.49	.96	.83	1.79	2.87	92.72
8R-188	Cannel coal ^c	79.93	6.44	1.69	1.05	4.55	6.34	83.74

^a Whole coal, ca. 25 per cent vitrain (see text).

^b Whole coal, over 90 per cent vitrain (see text).

^c Whole coal.

Table 3. Results of dehydrogenation with phenanthridine as vehicle and 1 per cent palladium on calcium carbonate catalyst^a

Run No.	Vitrain	C, maf	Per cent		H evolved, ml/g ^d	H/C atomic	O/C atomic
			H ₂ evolved ^b	H/100 C evolved ^c			
9R-32	Beulah-Zap (Zap Mine)	67.81	26.6	26.1	165	0.981	0.278
8R-190	Kincade	68.19	26.1	21.9	140	.842	.284
9R-40	Beulah-Zap (Beulah Mine)	68.93	39.2	38.0	244	.969	.258
9R-42	Roland-Smith (Wyodak)	70.19	26.7	27.2	178	1.016	.229
9R-3	Dietz (Big Horn)	70.84	33.9	28.9	191	.852	.238
9R-134	Laramie (Washington)	71.54	24.5	22.8	152	.928	.218
9R-132	Pioneer Canon No. 1	72.54	30.6	26.9	182	.879	.205
8R-156	Rock Springs	73.70	31.2	26.3	181	.842	.193
8R-161	Illinois No. 6 (Green Diamond)	75.65	39.0	34.8	246	.892	.149
8R-162	Illinois No. 6 (Mecco)	76.06	38.9	33.4	238	.860	.151
9R-34	No. 11 (Rainbow No. 7)	76.52	43.6	38.7	277	.888	.147
8R-184	Illinois No. 7 (Harmatten)	76.58	44.0	36.6	262	.832	.147
9R-41	Liberty	77.65	45.1	42.6	310	.946	.132
8R-186	Illinois No. 6 (Orient No. 3)	79.14	37.1	29.4	217	.792	.119
8R-159	Kentucky No. 9 (Pleasant View)	79.34	39.1	35.1	260	.899	.105
8R-158	Kentucky No. 9 (DeKoven)	80.69	35.4	31.2	235	.881	.0922
8R-143	Pittsburgh (Bruceton)	83.09	37.4	30.0	232	.802	.0786
8R-172	Pittsburgh (Bruceton)	83.09	37.1	29.8	231	.802	.0786
8R-147	Pittsburgh (Bruceton)	83.09	35.7	28.7	222	.802	.0786
8R-149	Pittsburgh (Bruceton)	83.09	37.0	29.7	230	.802	.0786
8R-160	Pond Creek (Majestic)	83.74	33.5	26.6	207	.793	.0762
8R-187	Powellton (Elk Creek No. 1)	85.05	35.3	26.3	209	.745	.0629
8R-157	Eagle (Kopperston)	86.19	29.0	22.6	182	.779	.0497
8R-165	Sewell (Lochgelley)	86.42	27.4	19.8	160	.723	.0529
8R-176	Lower Freeport (Coal Valley No. 7)	87.28	26.3	18.9	154	.718	.0415
8R-175	Lower Kittanning (Melcroft)	87.37	28.3	19.7	160	.698	.0384

Continued

Run No.	Vitrain	C, maf	Per cent H ₂ evolved ^b	H/100 C evolved ^c	H evolved, ml/g ^d	H/C atomic	O/C atomic
8R-167	Lower Banner (Buccaneer)	88.39	24.0	17.5	144	.730	.0350
8R-164	Sewell (Marianna)	88.93	22.3	15.1	126	.676	.0321
8R-174	Beckley (Maben)	88.94	21.6	13.8	115	.638	.0299
8R-166	Sewell (Crab Orchard)	89.29	19.6	13.3	110	.678	.0307
9R-133	Lower Hartshorne	89.52	20.5	13.6	114	.665	.0248
8R-185	Upper Kittanning (Stineman No. 10)	90.07	21.3	14.0	118	.658	.0215
8R-181	Pocahontas No. 4 (McAlpine)	90.27	19.1	11.6	99	.613	.0230
8R-183	Lower Kittanning (Toth)	90.47	21.2	13.8	116	.650	.0206
8R-182	Pocahontas No. 3 (Buckeye No. 3)	90.96	22.5	14.0	119	.621	.0182
9R-119	Semianthracite (Bernice)	89.99	1.0	.5	5	.516	.0353
9R-118	Semianthracite (Western Middle)	90.55	2.4	1.2	11	.526	.0249
8R-189	Dorrance anthracite	92.72	0.0	0.0	0	.326	.0237
8R-188	Cannel coal	83.74	30.2	29.0	227	.960	.0595

^a All runs used catalyst lot C-2842 except for 8R-147, 149 which used lot 7902.
All runs used magnetic stirring. Samples were -200 mesh.

^b Per cent of hydrogen in starting material which is evolved as H₂ gas.

^c Atoms of hydrogen evolved as H₂ gas per 100 C atoms in starting material.

^d Milliliters of hydrogen gas evolved per gram of m.a.f. starting material.

In Table 2, the four runs on Pittsburgh (Bruceton) vitrain gave some idea of the reproducibility which can be expected. The first two runs are with one batch of catalyst, the second pair is with another batch of catalyst. (All of the other runs listed were made with the same catalyst used for the first pair on Bruceton vitrain.)

Figure 1 shows the hydrogen evolution as a function of carbon content (maf) of the starting vitrain. In discussing this, it should be noted that the system used for classification of coals according to rank^{19,20} is not based upon the chemical structure of the coal. Instead, rank classification is based partly upon fixed carbon (which is not directly related to the carbon content determined by a standard combustion analysis), partly upon volatile matter (which again does not correspond to any usual chemical determination), partly upon Btu content (which of course is related, but in no specific way, to chemical composition), and partly upon agglomeration properties. In Figure 1, for 24 vitrains, all obtained from coals ranging in rank from high volatile C bituminous to low-volatile bituminous, the data scatter about a reasonably smooth curve, in which the hydrogen evolution decreases gradually as the carbon content increases from 75.7 percent maf to 91.0 percent maf. Three other points, for semianthracite and anthracite, suggest that the hydrogen evolution decreases rapidly for ranks above low-volatile bituminous, reaching zero for an anthracite. This is reasonable; it is generally agreed that the coalification process involves an increase in the aromatic nature of the coal, and it is not surprising that, by the time anthracite is reached, there are no hydroaromatic structures remaining in the coal.*

The low rank vitrains do not seem to fall on the same curve defined by the vitrains from bituminous coals. Two of the three lignite vitrains and all five of the subbituminous vitrains fall well below the band established by the bituminous vitrains. This difference can be brought out more clearly by plotting the hydrogen evolved (H/100 C) against the atomic H/C ratio, or even better, against the atomic O/C ratio, of the vitrain. These two graphs are shown in Figures 2 and 3. In Figure 2, it can be seen that a plot of H/100 C against H/C ratio gives a fairly good straight line for the 24 bituminous vitrains. The solid line shown is a least squares straight line for these 24 points. The equation of the line is given by: $H/100 C = 93.11 (H/C) - 46.68$. For the straight line, the standard error of estimate is 2.54; the multiple correlation coefficient is 0.966. The dashed lines on either side of the solid line are at distances of twice the standard error of estimate; this means that 95 percent of the points should lie within the two dashed lines. Put in other words, if a point lies outside the area between the two lines formed by the twice standard error, there is only a probability of 1/20 that this point belongs with the set of data used to draw the least squares line. It can be seen that one subbituminous falls within the area; one lignite and one subbituminous fall barely outside; and the other three subbituminous and two lignites fall outside of the area.

*Cannel coal is included on the graph for the sake of completeness; it is an atypical whole coal and will not be discussed.

Figure 3 is a similar plot of H/100 C against the O/C ratio. For the 24 bituminous vitrains, the equation of the least squares straight line is: $H/100 C = 190.5 (O/C) + 10.51$. For this straight line, the standard error of estimate is 3.20; the multiple correlation coefficient is 0.946. Since the oxygen analysis is by difference, it is subject to a larger error than are the other analyses. The O/C ratio is therefore less accurate than the H/C ratio, and the increased standard error and decreased multiple correlation coefficient for the O/C curve (as compared with the H/C curve) is to be expected.

In Figure 3, it is seen that all of the lignite and subbituminous points fall well outside the area of twice the standard error. For any one lignite point, the probability of it belonging with the bituminous straight line is 1/20; therefore, it might be said that the probability of all three lignite vitrains belonging to the bituminous set is 1/8000, or 0.000125. There is an even lower probability that all five subbituminous vitrains belong with the bituminous set. It is significant that all eight points fall on the same side of the least squares straight line.

Another approach to the data has been to find the least squares straight line for the combined 32 points (24 bituminous, 5 subbituminous, and 3 lignites). The equation for this line (which is not shown in any figure) is: $H/100 C = 59.1 (O/C) + 18.1$. For this line, the standard error of estimate has increased to 7.25; the multiple correlation coefficient has decreased to 0.581. The standard error has thus more than doubled, and the multiple correlation coefficient has decreased greatly. This again indicates that the subbituminous and lignite vitrains are not part of the bituminous group.

From the above discussion we may draw the following conclusion: that there is a fundamental chemical difference between bituminous coals on the one hand, and subbituminous coals and lignites on the other hand. This difference manifests itself in the amount of hydrogen gas produced by catalytic dehydrogenation in the presence of a solvent. This, in turn, must be related to the general structure of the coal and in particular to its hydroaromaticity. Thus, although a high volatile C bituminous coal and a subbituminous A coal are distinguished from each other solely on the basis of calorific limits and agglomerating properties^{19,20}, there must nevertheless be a real difference in their chemical structure.

One may wonder why this demarcation is more obvious in the O/C plot (Figure 3) than it is in the H/C plot (Figure 2). One possible explanation is that for the entire bituminous group of coals, the hydrogen varies only slightly, being in the range of 4.5 to 6.0 percent; the carbon, however, varies from 68 to 90 percent. On the other hand, the oxygen and carbon values both vary considerably, and they vary in opposite directions; so that the O/C plot is probably a more sensitive indication of the structural change.

We come now to a consideration of the reasons for the sharp difference between the bituminous coals and lower rank coals, as shown by dehydrogenation. It is generally assumed that one of the major reactions of the coalification process is aromatization²¹. A decreasing yield of hydrogen obtained from coals of increasing rank can be simply explained on the basis of the higher rank coals being more aromatic. The low yield of hydrogen from low rank coals remains to be explained, however. At first thought, one is inclined to assume that a process of continual aromatization must by its very nature also be a process of dehydroaromatization; that is, aromatization should cause loss of

hydroaromatic structures. This is not true, however, because aromatization may take place by changes in structures which are not themselves hydroaromatic. A schematic representation (Figure 4) illustrates a possible series of reactions for this process. The \textcircled{R} portion is intended to represent the bulk of a coal molecule, with attention focused on the ring system attached to it. In structure (I), there is no hydroaromatic system (as per the definition given above) and no normal dehydrogenation can take place; the angular methyl group slows aromatization³, since it must either migrate or be eliminated before dehydrogenation can take place. If the natural coalification process involves an aromatization* we may presume that the methyl group either migrates from the angular 9-position, which permits easy dehydrogenation to (II) and then further dehydrogenation to (IV); or alternatively the methyl group is eliminated from (I) as methane, which permits dehydrogenation to (III) and then further dehydrogenation to (V). We may consider (I) as corresponding to lignites and sub-bituminous coals; high hydrogen but no hydroaromatic structures. We may consider (II) and (III) as corresponding to bituminous coals; in the process of coalification (I \rightarrow II + III) there has been simultaneous formation of aromatic structures and of dehydrogenatable hydroaromatic structures. Thus we have a model for a process in which a non-hydroaromatic structure (I) is partly aromatized to give aromatic structures which also contain hydroaromatic rings. In a continuation of the coalification process, (II) and (III) are aromatized to (IV) and (V), which are completely aromatic (anthracite) and hence cannot give any hydrogen gas upon treatment with a dehydrogenation catalyst. This greatly simplified series of reactions, I \rightarrow II \rightarrow IV and I \rightarrow III \rightarrow V, offers a model for the seemingly peculiar situation in coal, where very low rank coals yield less hydrogen than do some higher rank, more aromatic coals.

It must be emphasized that the mechanism in Figure 4 is very schematic, is capable of many variations, and that several of these variations might proceed simultaneously. For example, the blocking group in the 9-substituted decalin structure (I) need not be methyl; it could be other groups, e.g., carboxyl. The blocked low rank structure (I) could be a 1,1-disubstituted cyclohexane type, which would undergo a similar series of transformations, or it could be a bridged six membered ring of the bicycloheptane type.

While this theory is not without its attractiveness, it may be asked whether coal can reasonably be expected to contain blocked structures of the type of (I). Coal is usually considered to arise by changes in the lignin and perhaps in the cellulose of the plant material which is its precursor²¹. Neither lignin nor cellulose contains polycyclic structures of the type of (I). Lignin contains benzene rings with reactive side chains. It is quite possible to visualize formation of condensed ring systems from cellulose, from lignin, or from an interaction of the two. Further, many plants contain appreciable amounts of other materials[†] more closely related in structure to (I). These include tricyclic diterpenes (abietic acid types), pentacyclic triterpenes (amyrin types), and tetracyclic sterols (stigmaterol and lanosterol types), which contain 1,1-dimethyl groups and angular methyl groups; and bicyclic terpenes

*For the purpose of this discussion we neglect the detailed mechanism of the coalification process and do not consider the loss of oxygen (perhaps as water) which takes place during coalification.

† The structures of some of these compounds are shown in Figure 5.

(pinene and camphane types) which contain bridged rings and 1,1-dimethyl groups. Also to be considered are some of the complex polycyclic alkaloids containing heterocyclic nitrogen, which occur in large amounts in some plants. It is possible that compounds of these types play a more important part in the coalification process than has heretofore been realized.

It remains to consider three possible sources of error in the hydrogen values obtained, all of which we believe are minor. These are interaction of the coal with the vehicle; cross-linking of coal structures during dehydrogenation, with formation of hydrogen*; and effect of phenolic groupings in the coal. It is known that the vehicle reacts with the coal, and it has so far proven impossible to remove all of the phenanthridine from a dehydrogenated coal¹². Obviously, the reaction: $\text{Coal-H} + \text{Vehicle-H} \rightarrow \text{Coal} \sim \text{Vehicle} + \text{H}_2$ would lead to a high value for hydrogen liberated. However, vehicle-vitrain blanks have been shown to be negligible and vehicle-catalyst blanks have been deducted, although this does not preclude interaction between coal and vehicle in the presence of catalyst. In addition, a reaction of the type: $\text{Coal-H} + \text{Vehicle-H} \rightarrow \text{H-Coal} \sim \text{Vehicle-H}$ would also account for the impossibility of removing vehicle from dehydrogenated coal and yet would not lead to hydrogen formation. Further experiments may throw some light on this process. We do know that one vehicle (1-azapyrene) liberates large amounts of hydrogen when heated only with a catalyst and that at least one other vehicle (2-azafluoranthene) gives very high values for hydrogen evolution from coal¹¹ which are almost certainly incorrect. Nevertheless, there is no real reason to believe that the phenanthridine contributes significantly to the evolved hydrogen, although this possibility must be kept in mind. Second, there is the question of "cross-linking," a somewhat vague term implying chemical reaction between two coal platelets. Here again, there are two possible reactions analogous to the two given above:



The first of these would lead to extra evolution of hydrogen, the second would not. The insolubilization of the coal which takes place during dehydrogenation could be used as an argument in favor of cross-linking; however, one might reasonably expect the dehydrogenated coal to be less soluble than the starting material in any case. Third, we have found that certain phenolic compounds yield hydrogen, probably by reactions of the type



This reaction can be eliminated by the use of the silyl ethers in place of the free phenols. However, there is some evidence (based on the dehydrogenation of silyl ethers of phenols) that the phenolic groups in coal give little or no hydrogen, and that this side reaction is of slight consequence in coal dehydrogenation.

*Infrared spectra did not yield any useful information. The presence of vehicle; the small number of protons; and the difficulty of grinding; all contribute to loss of spectral information. A similar situation was found by Friedel and Breger²² for a cross-polymerized coal formed by neutron irradiation.

REFERENCES

- 1 Lowry, H. H., editor, Chemistry of Coal Utilization (2 volumes). Wiley: New York, 1945
- 2 Lowry, H. H., editor, Chemistry of Coal Utilization, Supplementary Volume. Wiley: New York, 1963
- 3 Valenta, Z., in Technique of Organic Chemistry, volume XI, edited K. W. Bentley, pp. 581-642. Interscience: New York, 1963
- 4 Jackman, L. M., in Advances in Organic Chemistry, volume II, edited R. A. Raphael, E. C. Taylor, and H. Wynberg, pp. 329-366. Interscience: New York, 1960
- 5 Mazumdar, B. K., Chakrabartty, S. K., De, N. G., Ganguly, S., and Lahiri, A. Fuel, Lond. 1962, 41, 121
- 6 Peover, M. E. J. Chem. Soc., Lond. 1960, 5020
- 7 Mazumdar, B. K., Bhattacharyya, A. C., Ganguly, S., and Lahiri, A. Fuel, Lond. 1962, 41, 105; Peover, M. E., Fuel, Lond. 1962, 41, 110
- 8 Mazumdar, B. K., Choudhury, S. S., and Lahiri, A. Fuel, Lond. 1960, 39, 179
- 9 Shishido, K. and Nozaki, H. J. Soc. Chem. Ind. Japan 1944, 47, 819. Eberhardt, M. K. Tetrahedron 1965, 21, 1383. Eberhardt, M. K. Tetrahedron 1965, 21, 1391. Raley, J. H., Mullineaux, R. D. and Bittner, C. W. J. Am. Chem. Soc. 1963, 85, 3174. Mullineaux, R. D. and Raley, J. H. J. Am. Chem. Soc. 1963, 85, 3178. Slauch, L. H., Mullineaux, R. D. and Raley, J. H. J. Am. Chem. Soc. 1963, 85, 3180. King, R. W. Hydrocarbon Processing 1966, 45, 189
- 10 Rabindran, K. and Tilak, B. D. Proc. Indian Acad. Sci. 1953, 37A, 557
- 11 Raymond, R., Wender, I. and Reggel, L. Science 1962, 137, 681
- 12 Reggel, L., Wender, I., and Raymond, R. Fuel, Lond. 1964, 43, 229
- 13 Baxter, R. A., Ramage, G. R. and Timson, J. A. J. Chem. Soc. (Suppl. Issue No. 1) 1949, S30
- 14 Albert, A., Brown, D. J. and Duewell, H. J. Chem. Soc. 1948, 1284
- 15 Horning, E. C., Horning, M. G. and Walker, G. N. J. Am. Chem. Soc. 1948, 70, 3935
- 16 Grob, C. A. and Hofer, B. Helv. Chim. Acta. 1952, 35, 2095
- 17 Horrobin, S. and Young, R. J. British Patent 745,400, 1956; Chem. Abstr. 1956, 50, 16875c
- 18 Fieser, L. P. and Fieser, M. Advanced Organic Chemistry p. 645. Reinhold: New York, 1961
- 19 Ode, W. H. and Frederick, W. H. United States Department of the Interior, Bureau of Mines, 'The International Systems of Hard-Coal Classification and Their Application to American Coals.' Rept. of Inv. 5435, pp. 3-12, U. S. Government Printing Office, 1958
- 20 1965 Book of ASTM Standards, Part 19. Gaseous Fuels; Coal and Coke. Page 74. American Society for Testing and Materials: Philadelphia, Pa.
- 21 Van Krevelen, D. W. Coal, pp. 101-109, 445-452. Elsevier: Amsterdam, 1961
- 22 Friedel, R. A. and Breger, I. A. Science 1959, 130, 1762-1763

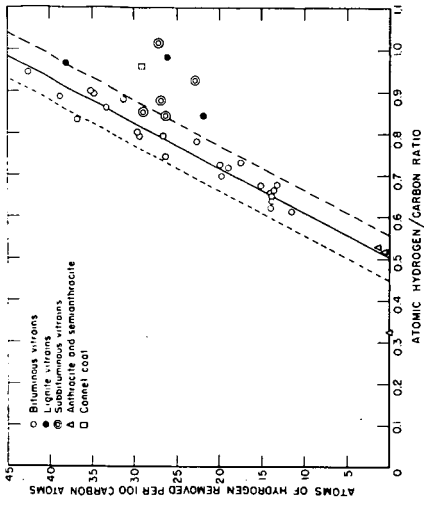


Figure 2.-Dehydrogenation of vitrains with one percent palladium on calcium carbonate catalyst, phenanthridine vehicle, plotted as a function of the atomic H/C ratio. The solid line is the least squares straight line for the 24 bituminous vitrains. The dashed lines are drawn at a distance of twice the standard error of estimate.

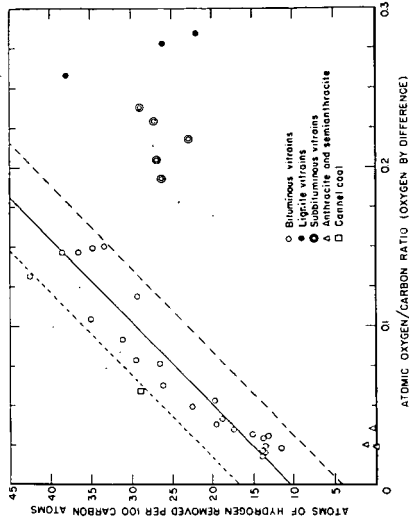


Figure 3.-Dehydrogenation of vitrains with one percent palladium on calcium carbonate catalyst, phenanthridine vehicle, plotted as a function of the atomic O/C ratio (oxygen analysis by difference). The solid line is the least squares straight line for the 24 bituminous vitrains. The dashed lines are drawn at a distance of twice the standard error of estimate.

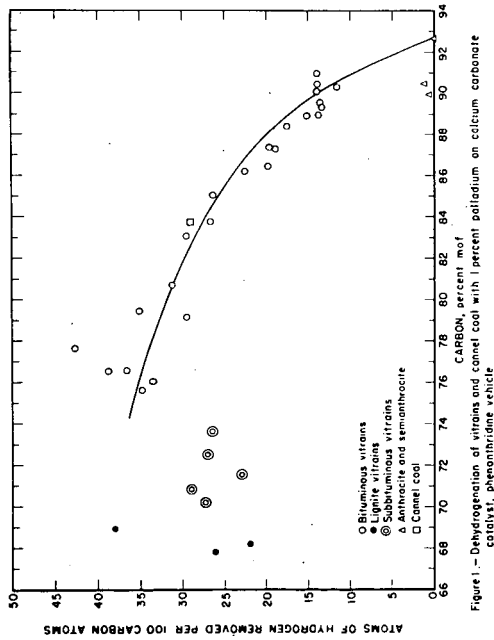


Figure 1.-Dehydrogenation of vitrains and cannel coal with 1 percent palladium on calcium carbonate catalyst, phenanthridine vehicle

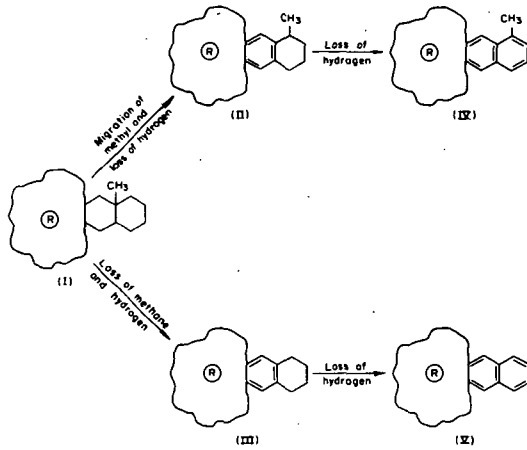


Figure 4.-Schematic representation of the coalification process.

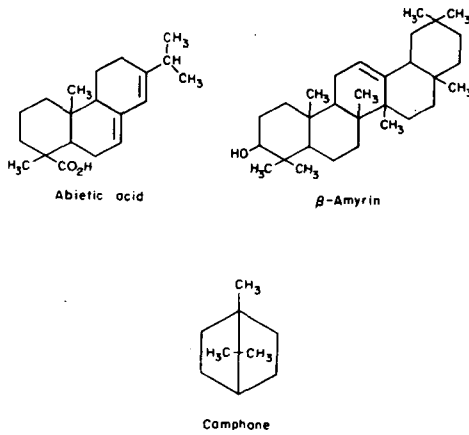


Figure 5-Structures of compounds found in plants which may be coal precursors (see text)

A RAPID, SIMPLE METHOD FOR THE DETERMINATION
OF THE THERMAL CONDUCTIVITY OF SOLIDS

Neal D. Smith
Fay Fun
Robert M. Visokey

UNITED STATES STEEL CORPORATION
Research Center
Monroeville, Pennsylvania

The rational design of equipment such as shaft coolers, heaters, and rotary kilns for the heating and cooling of solids requires that the thermal properties of the solids be known. Thermal conductivity is one of these properties that to measure necessitates elaborate equipment and time-consuming techniques.

A rapid, simple method has been developed for determining the thermal conductivity of solids. The solids can be either porous or non-porous and of either high or low conductivity. If high-conductivity materials are tested, then both the thermal conductivity and heat capacity can be simultaneously measured by the method.

The procedure involves preparing a cylindrical briquette of the test solid that has a thermocouple located in the center. This briquette is heated to a constant temperature after which it is suspended in an open-end glass tube and cooled by a known flow of nitrogen or any other nonreactive gas. The thermal conductivity is then computed from a digital computer comparison of the cooling curves for the test solid versus a reference solid of known thermal properties and similar size that has undergone the same heating and cooling cycle. The method was validated by using the known thermal properties of lead, aluminum, and silver and computing the theoretical cooling curves. The theoretical curves were in close agreement with the experimentally measured cooling curves for these materials.

Theory

The mathematical basis for determining thermal conductivity by the described method is discussed in a paper by Newman¹⁾ and is summarized as follows. Consider a cylindrical briquette as shown in Figure 1. The differential equation for unsteady state heat transfer by conduction in the x-direction is (see nomenclature for definition of the variables):

$$\frac{\partial t}{\partial \theta} = \alpha \left(\frac{\partial^2 t}{\partial x^2} \right) \quad (1)$$

For a briquette of thickness $2a$, the central plane being at $x = 0$ and assuming:

- 1) uniform temperature at the start of cooling of the initially hot briquette

then $t = t_0$ when $\theta = 0$ (2)

- 2) the final temperature of the briquette will be the temperature of the surroundings:

therefore $t = t_s$ when $\theta = \infty$ (3)

- 3) there is no heat flow across the central plane because of symmetry:

consequently $-k \left(\frac{\partial t}{\partial x} \right) = 0$ at $x = 0$ (4)

The heat balance on the briquette surface is made by equating heat transferred to the surface by conduction with heat transferred from the surface by convection. In differential form, the heat balance is:

$$-k \left(\frac{\partial t}{\partial x} \right) = h (t - t_s) \text{ at } x = \underline{a} \quad (5)$$

Newman¹⁾ showed that the solution to Equations (1) through (5) expressed in terms of a dimensionless temperature ratio Y_x is:

$$Y_x = \frac{t - t_s}{t_0 - t_s} = 2 \sum_{n=1}^{\infty} A_n e^{-(\beta_n^2 X_a)} \cos(\beta_n \frac{x}{a}) \quad (6)$$

where $A_n = \frac{m_a}{(1 + \beta_n^2 m_a^2 + m_a) \cos \beta_n}$ and

β_n are defined as the first, second, third, etc., roots of the transcendental equation:

$$\beta_n \tan \beta_n - 1/m_a = 0 \quad (7)$$

The surface to solid thermal resistance ratio, m_a , is defined as:

$$m_a = k/ha \quad (8)$$

and X_a is defined as: $X_a = \alpha \theta / a^2$ (9)

where the thermal diffusivity is: $\alpha = k/\rho C_p$ (10)

Similarly, considering radial heat transfer, the radial briquette heat balance is

$$\frac{\partial t}{\partial \theta} = \alpha \left[\frac{\partial^2 t}{\partial r^2} + \frac{1}{r} \frac{\partial t}{\partial r} \right] \quad (11)$$

The initial condition equation is:

$$t = t_0 \text{ when } \theta = 0 \quad (12)$$

The final temperature equation is:

$$t = t_s \text{ when } \theta = \infty \quad (13)$$

The boundary condition equations are:

$$-k \left(\frac{\partial t}{\partial r} \right) = 0 \text{ at } r = 0 \quad (14)$$

and
$$-k \left(\frac{\partial t}{\partial r} \right) = h (t-t_s) \text{ at } r = R \quad (15)$$

Solving Equations (11) through (15) gives:

$$\frac{t - t_s}{t_o - t_s} = 2 \sum_{n=1}^{\infty} A_n e^{-(\beta_n^2 X_r)} J_0(\beta_n \frac{r}{R}) = Y_r \quad (16)$$

where

$$A_n = \frac{m_r}{(1 + \beta_n^2 m_r^2) [J_0(\beta_n)]} \quad (17)$$

and β_n are the first, second, third, etc., roots of the equation:

$$\beta_n J_1(\beta_n) - 1/m_r J_0(\beta_n) = 0 \quad (18)$$

The surface to solid thermal resistance ratio, m_r is

$$m_r = k/hR \quad (19)$$

and
$$X_r = \alpha \theta / R^2 \quad (20)$$

The complete differential equation for the case shown in Fig. 1 is:

$$\frac{\partial t}{\partial \theta} = \alpha \left(\frac{\partial^2 t}{\partial r^2} + \frac{1}{r} \frac{\partial t}{\partial r} + \frac{\partial^2 t}{\partial x^2} \right) \quad (21)$$

and the solution to Equation (21) is:

$$Y = \frac{t - t_s}{t_o - t_s} = Y_r \cdot Y_x \quad (22)$$

If the center temperature defined at $r = 0$, $x = 0$ is t_c , then Equation (22) becomes:

$$Y_c = \frac{t_c - t_s}{t_o - t_s} = Y_r \cdot Y_x \quad (23)$$

where Y_r and Y_x are evaluated at $r = 0$ and $x = 0$.

The preceding mathematical analysis shows that the rate of cooling, or change in center temperature for a cylindrical briquette is a function of time (θ), density (ρ), thermal conductivity (k), the surface heat transfer coefficient (h), specific heat (C_p) and the briquette dimensions as expressed by Equation (23).

The experimental technique can now be described in terms of the previous discussion. If the change in center temperature with time is measured experimentally for a material of known thermal and physical properties (standard briquette), the surface heat transfer coefficient can be calculated from Equation (23), since it is the only unknown.

The surface heat transfer coefficient (h) is a function of the flow rate of the cooling gas and the geometry and size of the briquette. It is independent of all other physical, thermal, or chemical properties of the briquette. Therefore, any other briquette having similar dimensions and cooled at the same flow rate will have the same value for (h).

Once (h) has been determined using the standard briquette, the thermal conductivity of any test material can be determined from Equation (23) since all other variables are known.

A computer program has been written which through an iterative process determines the best value of (h) which makes the calculated values for the dimensionless temperature ratio equal to the experimental values obtained when the standard briquette is cooled.

With (h) determined, another computer program is run for the test specimen. Thermal conductivity is now the unknown variable and through another iterative scheme, the best value for (k) that makes the calculated and experimental values for the temperature ratios equal is found.

The input data for both programs consist of density, specific heat, time, briquette dimensions, and several experimental values for the temperature ratio. The output from the first program (standard) is the best value for (h). Using this value for (h), the second program used to determine the k value for any test material. If a highly conductive material is tested, then it is possible to determine its heat capacity since the solid thermal resistance will be small compared to the surface thermal resistance. A transient heat balance can be written for the test solid cooling in a stream of coolant gas.

$$V\rho C_p \frac{dt}{d\theta} = hA (t - t_s) \quad (24)$$

In the above equation, $t = t_c$ since the thermal gradient in the solid is neglected. Integrating Equation (24) and using the dimensionless temperature ratio, Y_c gives:

$$Y_c = \exp -(hA/\rho C_p V)\theta \quad (25)$$

Thus, if the internal solid thermal resistance is negligible, a plot of the experimental Y_c versus θ data on semilog paper should be linear as shown by Equation (25). The heat capacity, C_p , can be calculated from the slope of the line for Y_c versus θ since (h) is the same as for the standard briquette and the density, ρ , and total surface area, A , for the test material are also known.

Materials and Experimental Work

A primary advantage of the transient technique for determining thermal conductivities is the ease and swiftness with which the experiment can be conducted.

In so far as sample preparation is concerned, any solid that can be briquetted, cast, or fabricated around a centrally located rigid.

thermocouple ($x = 0$; $r = 0$) may be tested. Finished test sample cylinders should be approximately one inch in diameter, and one-half inch in height; however, other dimensions can be used.

Experimental Apparatus

The experimental apparatus (see Figure 2) consists simply of a 3-inch diameter glass tube approximately 3 feet in length. One end of the tube is completely stoppered except for a one-half inch circular opening through which the coolant gas flows. The other end of the tube is open to the atmosphere. A small electric furnace is used to heat the briquette, and an automatic single point temperature recorder connected to the embedded thermocouple is used to measure the center temperature of the briquette.

Experimental Procedure

The experimental procedure is the same for both the standard and test briquettes. Either the standard (aluminum was chosen since its thermal properties are well established), or the test briquette is connected to the temperature recorder by way of the thermocouple leads. The briquette is heated until the center temperature has reached a constant, predetermined value. The briquette is then quickly removed from the furnace and suspended in the cooling tube with the cooling gas flowing at a constant rate. The briquette is usually cooled to the temperature of the cooling gas within 20 minutes.

Data Processing

For the standard briquette, the experimental dimensionless temperature ratio versus time data points for the standard briquette along with the known thermal properties are used to calculate the surface coefficient, h , in the following manner. A digital computer program is written to compute Y_c from Equations (6) through (23). By iteration and assuming various values of (h), the computed values of Y_c can be made to converge on each of selected experimental Y_c versus θ data points. Thus, for a selected data point, the best experimental (h) is that which when used in Equations (8) and (19) results in equal values for the computed and experimental Y_c values.

For low conductivity test materials, the same method is used to determine the best experimental value of k by using the h determined for the standard and the other properties of the test material. If the test material is a good conductor as discussed in the theory section, then experience has shown that h should be computed from the experimental cooling curve and then this value is used to compute k by the same method as for low conductivity test materials.

Discussion and Results

Three briquettes of aluminum, lead and silver were made to test the validity of the experimental technique since their thermal properties were available from the literature as shown in Table I.

Sintered, dense hematite (Fe_2O_3) and a briquette of porous carbon made from a partially devolatilized coal were used as test materials. For these materials, all properties except the thermal conductivities shown in Table I were previously measured. Cooling curves for each briquette were measured for a nitrogen flow rate of 0.9 scfm. Surface heat transfer coefficients for lead, silver and aluminum were calculated by the method discussed in the data processing section. For these materials, the literature conductivity values were used to calculate the surface coefficient. Table I shows that the calculated or experimental h values for each metal are nearly identical. This result is consistent with the theoretical basis of the experiment and may be considered as establishing the validity of the method. Also as additional evidence, aluminum was chosen as the standard and k values for lead and silver were calculated using the h value for aluminum. Table I shows that the calculated or experimental k values were within 0.5 percent of the literature values. The conductivities for hematite and porous carbon were calculated using aluminum as the standard. Figure 3 shows the experimental data points with the solid lines calculated from the theory. Note that the line for the carbon is curved whereas those for the metals and hematite are linear. As discussed previously, a linear cooling curve is obtained if the surface to solid thermal resistance ratios are relatively large. Note that for the metals, lead which has the lowest conductivity and thermal diffusivity cooled the fastest. This result is explained by examination of eqn. (25) which shows that for similar gas flows and briquette dimensions, the rate of cooling for different materials is determined by the heat content, ρC_p . It can be seen in Table I that the heat content for lead is the lowest of all metals tested.

Summary

A rapid, simple method for determining thermal conductivity for a solid has been developed. The solid can be either porous or non-porous and of either high or low conductivity. If high conductivity materials are tested, then both conductivity and heat capacity can be simultaneously measured from one cooling experiment. The method was validated by using the known thermal properties of lead, aluminum, and silver and the experimental cooling curves in a comparison with the computed results.

References

1. Newman, A. B., Industrial and Engineering Chemistry, Vol. 28, 1936, pp. 545-548.

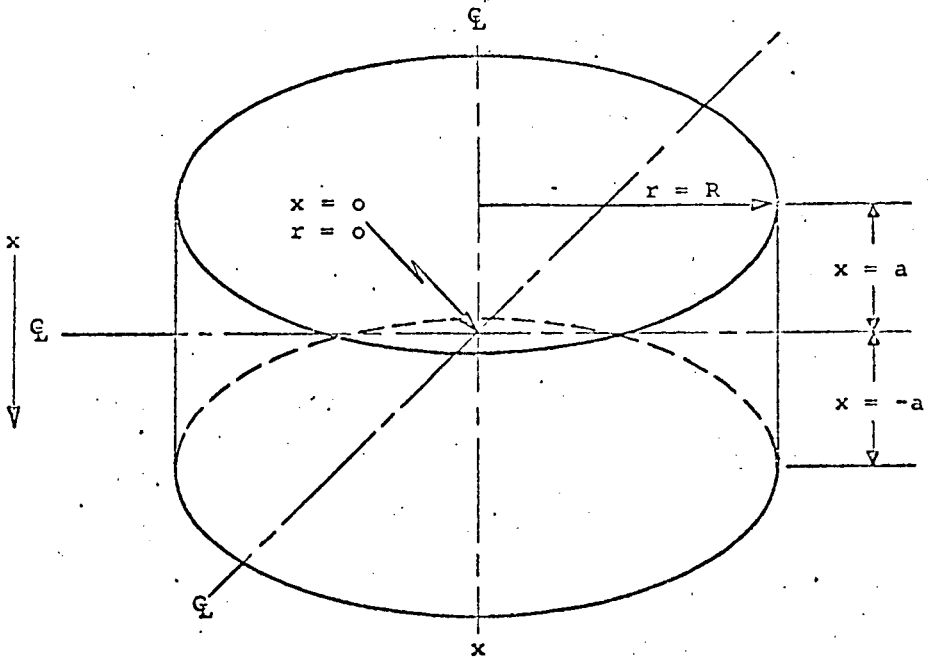
Nomenclature

- a = Half height of briquette; ft
 A = Area; ft^2
 A_n = Coefficient in infinite series solution for temperature distribution in briquette
 C_p = Specific heat; $\text{BTU/lb } ^\circ\text{F}$
 h = Surface heat transfer coefficient; $\text{BTU/hr ft}^2 \text{ } ^\circ\text{F}$
 k = Thermal conductivity; $\text{BTU/hr ft}^2 \text{ } ^\circ\text{F/ft}$
 m_a = Axial surface resistance; dimensionless
 m_r = Radial surface resistance; dimensionless
 R = Maximum radius of briquette; ft
 r = Radius of briquette; ft
 t = Temperature; $^\circ\text{F}$
 t_c = Temperature at center of briquette; $^\circ\text{F}$
 t_o = Initial temperature of briquette; $^\circ\text{F}$
 t_s = Temperature of cooling gas; $^\circ\text{F}$
 x = Distance of direction; ft
 X_a = $\frac{\alpha\theta}{a^2}$ Dimensionless time parameter for axial component
 X_r = $\frac{\alpha\theta}{R^2}$ Dimensionless time parameter for radial component
 Y_x = Symbol for temperature ratio, axial component; dimensionless
 Y_r = Symbol for temperature ratio, radial component; dimensionless
 α = $(k/\rho C_p)$ Thermal diffusivity; ft^2/hr
 θ = Time; minutes or hours
 ρ = Density; lb/ft^3

Table I
THERMAL AND PHYSICAL PROPERTIES FOR THE BRIQUETTES

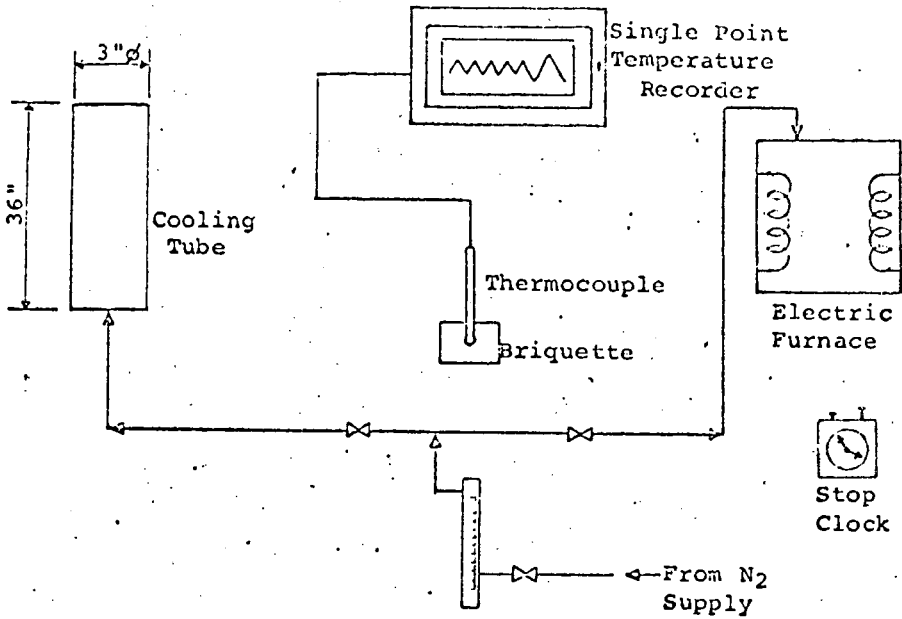
	Aluminum	Silver	Lead	Hematite	Porous Carbon
a	.01842	.02059	.01842	.01842	.01958
R	.04208	.04210	.04117	.04208	.04121
ρ	168.50	655.20	707.43	306.00	75.0
C_p	.2273	.0578	.0306	.2090	.2360
ρC_p	38.30	39.31	21.65	63.95	17.70
h (experimental)	5.58	5.70	5.60	5.58	5.58
k (experimental)	Not Measured	240.3	18.99	12.10	.0307
k (literature)	121.7	240.0	19.00	none	none
α (experimental)	3.178*	6.113	.8770	.1892	.00173

*Average of literature sources



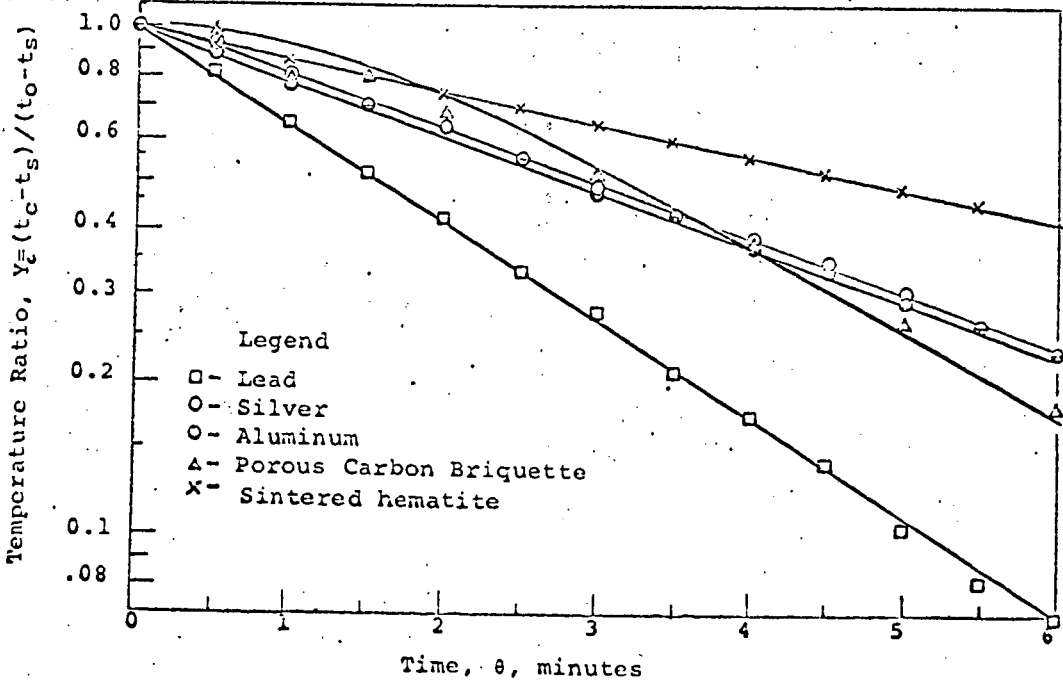
STANDARD CYLINDRICAL BRIQUETTE

Figure 1



EXPERIMENTAL APPARATUS

Figure 2



Theoretical Cooling Curves and Experimental Points for five Materials

Figure 3